

Quantum spin systems versus Schrödinger operators: A case study in spontaneous symmetry breaking

C. J. F. van de Ven¹, G. C. Groenenboom², R. Reuvers³, N. P. Landsman^{4*}

¹ Department of Mathematics, University of Trento, Trento, Italy.
Email: christiaan.vandeven@unitn.it.

² Theoretical Chemistry, Institute for Molecules and Materials, Radboud University,
Nijmegen, The Netherlands. Email: gerritg@theochem.ru.nl.

³ Department of Applied Mathematical and Theoretical Physics, University of Cambridge,
Cambridge, U.K. Email: r.reuvers@damtp.cam.ac.uk.

⁴ Institute for Mathematics, Astrophysics, and Particle Physics, Radboud University,
Nijmegen, The Netherlands. Email: landsman@math.ru.nl. *Corresponding author.*

Abstract

Spontaneous symmetry breaking (SSB) is mathematically tied to either the thermodynamic or the classical limit, but physically, some approximate form of SSB must occur *before* the limit. For a Schrödinger operator with double well potential in the classical limit, this may indeed be accomplished by the “flea” mechanism discovered in the 1980s by Jona-Lasinio et al. We adapt this mechanism to the Curie–Weiss model (as a paradigmatic mean-field quantum spin system), and also establish an unexpected relationship between this model (for finite N) and a discretized Schrödinger operator with double well potential.

Contents

1	Introduction	2
2	Reduction of the Curie–Weiss Hamiltonian	5
2.1	Tridiagonal form	5
2.2	Numerical simulations	7
3	From Curie–Weiss to a discretized Schrödinger operator	10
3.1	Locally uniform discretization	10
3.2	Link with a discrete Schrödinger operator	15
3.3	Link with a Schrödinger operator on $L^2([0, 1])$	23
4	The flea on Schrödinger’s Cat in the Curie–Weiss model	25
4.1	Perturbation of the Hamiltonian	26
5	Conclusion	31
A	Perron–Frobenius Theorem	32
B	Discretization	33

1 Introduction

At first sight, spontaneous symmetry breaking (SSB) is a paradoxical phenomenon: in *Nature*, finite quantum systems, such as ferromagnets, evidently display it, yet in *Theory* it seems forbidden in such systems. Indeed, for finite quantum systems the ground state of a generic Hamiltonian is unique and hence invariant under whatever symmetry group G it may have.¹ Hence SSB, in the sense of having a family of asymmetric ground states related by the action of G , seems possible only in infinite quantum systems or in classical systems (for both of which the arguments proving uniqueness, typically based on the Perron–Frobenius Theorem, break down. However, both are idealizations, vulnerable to what we call *Earman’s Principle* from the philosophy of physics:

“While idealizations are useful and, perhaps, even essential to progress in physics, a sound principle of interpretation would seem to be that no effect can be counted as a genuine physical effect if it disappears when the idealizations are removed.”
(Earman, 2004)

As argued in detail in Landsman (2013, 2017), the solution to his paradox lies in Earman’s very principle itself, which (contrapositively) implies what we call *Butterfield’s Principle*:

“there is a weaker, yet still vivid, novel and robust behaviour that occurs before we get to the limit, i.e. for finite N . And it is this weaker behaviour which is physically real.” (Butterfield, 2011)

Applied to SSB in infinite quantum systems, this means that some approximate and robust form of symmetry breaking should already occur in large but finite systems, *despite the fact that uniqueness of the ground state seems to forbid this*. Similarly, SSB in a classical system should be foreshadowed in the quantum system whose classical limit it is, at least for tiny but positive values of Planck’s constant \hbar . To accomplish this, it must be shown that for finite N or $\hbar > 0$ the system is not in its ground state, or equilibrium state, but in some other state having the property that as $N \rightarrow \infty$ or $\hbar \rightarrow 0$, it converges in a suitable sense (see Landsman (2017), Chapter 8 and Chapter 7, respectively) to a symmetry-broken ground state of the limit system, which is either an infinite quantum system or a classical system. Since the symmetry of a state is preserved under the limits in question (provided these are taken correctly), this implies that the actual physical state must already break the symmetry.² See

¹Similarly for equilibrium states at positive temperature, which are always unique.

²*Bogoliubov’s method of quasi-averages* looks superficially similar to this idea, see e.g. Wreszinski & Zagrebnov (2018). However, in Bogoliubov’s work the symmetry-breaking term seems to be a purely formal device which is removed after taking the appropriate limit. In our paper, as well as in the works just cited in the main text, the symmetry-breaking perturbations are physical and the essential point is that their importance grows in the limit, or, as phrased in van Wezel & van den Brink (2007): “The general idea behind spontaneous symmetry breaking is easily formulated: as a collection of quantum particles becomes larger, the symmetry of the system as a whole becomes more unstable against small perturbations.” The same is true as \hbar becomes smaller at fixed system size, and in fact the analogy between $N \rightarrow \infty$ and $\hbar \rightarrow 0$ is strong both mathematically and physically, as shown in this paper as well as in Landsman (2017).

Jona-Lasinio, Martinelli, & Scoppola (1981) for 1d Schrödinger operators with a symmetric double well potential in the classical limit, and (independently) Koma & Tasaki (1994), van Wezel (2007, 2008) and van Wezel & van den Brink (2007) for (general) quantum spin systems in the thermodynamic limit (also cf. Landsman, 2017). Since it plays a central role in what follows, we briefly recall the main point of Jona-Lasinio et al, later called the “flea on the elephant” (Simon, 1985) or the “flea on Schrödinger’s Cat” (Landsman & Reuvers, 2013). Consider the Schrödinger operator with symmetric double well, defined on suitable domain in $\mathcal{H} = L^2(\mathbb{R})$ by

$$h_{\hbar} = -\hbar^2 \frac{d^2}{dx^2} + \frac{1}{4}\lambda(x^2 - a^2)^2, \quad (1.1)$$

where $\lambda > 0$ and $a \neq 0$. For any $\hbar > 0$ the ground state of this Hamiltonian is unique and hence invariant under the \mathbb{Z}_2 -symmetry $\psi(x) \mapsto \psi(-x)$; with an appropriate phase choice it is real, strictly positive, and doubly peaked above $x = \pm a$. Yet the associated classical Hamiltonian

$$h_0(p, q) = p^2 + \frac{1}{4}\lambda(q^2 - a^2)^2, \quad (1.2)$$

defined on the classical phase space \mathbb{R}^2 , has a two-fold degenerate ground state: the point(s) (p_0, q_0) in \mathbb{R}^2 where h_0 takes an absolute minimum are of course $(p_0 = 0, q_0 = \pm a)$. In the algebraic formalism, where states are defined as normalized positive linear functionals on the C^* -algebra $A_0 = C_0(\mathbb{R}^2)$, the (pure) ground states are the *asymmetric* Dirac measures ω_{\pm} defined by

$$\omega_{\pm}(f) = f(p = 0, q = \pm a). \quad (1.3)$$

From these, one may construct the mixed *symmetric* state $\omega_0 = \frac{1}{2}(\omega_+ + \omega_-)$, which in fact is the limit of the (algebraic) ground state ω_{\hbar} of (1.1) as $\hbar \rightarrow 0$ (see Landsman, 2017, §7.1),³ where

$$\omega_{\hbar}(a) = \langle \psi_{\hbar}^{(0)}, a\psi_{\hbar}^{(0)} \rangle, \quad (1.4)$$

in terms of the usual ground state $\psi_{\hbar}^{(0)} \in L^2(\mathbb{R})$ of h_{\hbar} (assumed to be a unit vector). In order to have a quantum “ground-ish” state that converges to either one of the physical classical ground states ω_+ or ω_- rather than to the unphysical mixture ω_0 , we perturb (1.1) by adding an asymmetric term δV (i.e., the “flea”), which, however small it is, under reasonable assumptions localizes the ground state $\psi_{\hbar}^{(\delta)}$ of the perturbed Hamiltonian in such a way that $\omega_{\hbar}^{(\delta)} \rightarrow \omega_+$ or ω_- , depending on the sign and location of δV .⁴ In particular, the localization of $\psi_{\hbar}^{(\delta)}$ grows exponentially as $\hbar \rightarrow 0$.

In this paper, we realize the above scenario for SSB in the *Curie–Weiss model*,⁵ with

³Here ω_{\hbar} is defined as a normalized positive linear functional on the C^* -algebra $A_{\hbar} = B_0(L^2(\mathbb{R}))$ of compact operators on $L^2(\mathbb{R})$. The algebraic formalism is particularly useful for combining classical and quantum expressions.

⁴For example, if δV is positive and is localized to the right, then the relative energy in the left-hand part of the double well is lowered, so that localization will be to the left.

⁵This model falls into the class of homogeneous mean-field theories, see e.g. Bona (1988), Raggio & Werner (1989), and Duffield & Werner (1992), which differ from their short-range counterparts (which in this case would be the quantum Ising model) in that every spin now interacts with every other spin. This also makes the dimension d irrelevant (which marks a huge difference with short-range quantum spin models), and yet even the apparently simple Curie–Weiss model is extremely rich in its behaviour; see e.g. Allahverdyana, Balian, & Nieuwenhuizen (2013) for a detailed analysis (along quite different lines from our study), motivated by the measurement problem.

Hamiltonian

$$h_{\Lambda}^{\text{CW}} = -\frac{1}{2}|\Lambda|^{-1} \sum_{x,y \in \Lambda} \sigma_3(x)\sigma_3(y) - B \sum_{x \in \Lambda} \sigma_1(x), \quad (1.5)$$

where $\Lambda \subset \mathbb{Z}^d$ is finite, we take the spin-spin coupling to be $J = 1$, and B is an external magnetic field. This Hamiltonian has a \mathbb{Z}_2 -symmetry $(\sigma_1, \sigma_2, \sigma_3) \mapsto (\sigma_1, -\sigma_2, -\sigma_3)$, which at each site x is implemented by $u(x) = \sigma_1(x)$. The ground state of this model is unique for any $|\Lambda| < \infty$ and any $B \neq 0$, and yet, as for the double well potential, in the thermodynamic limit it has two degenerate ground states, provided $0 < B < 1$. As explained in Landsman (2017, §10.8), this limit actually defines a classical theory, with phase space $B^3 \subset \mathbb{R}^3$, i.e. the three-sphere with unit radius (and boundary $\partial B^3 = S^2$), seen as a Poisson manifold with bracket $\{x, y\} = z$ etc.), and Hamiltonian

$$h_0^{\text{CW}}(x, y, z) = -\frac{1}{2}z^2 - Bx. \quad (1.6)$$

The ground states of this Hamiltonian are simply its absolute minima, viz. (writing $\vec{x} = (x, y, z)$):

$$\vec{x}_{\pm} = (B, 0, \pm\sqrt{1-B^2}) \quad (0 \leq B < 1); \quad (1.7)$$

$$\vec{x} = (1, 0, 0) \quad (B \geq 1), \quad (1.8)$$

which lie on the boundary S^2 of B^3 (note that the points \vec{x}_{\pm} coalesce as $B \rightarrow 1$, where they form a saddle point). Thus we seem to face a similar paradox as for the double well (Landsman, 2013).

Even if one is familiar with the example of SSB in the classical limit of the double well (as just reviewed), the case of the Curie–Weiss model is far from trivial, and our attempts to resolve the (apparent) paradox in question have led us to a deeper understanding of the model altogether. In §2 we show that due to permutation invariance, the ground state of the $1d$ Curie–Weiss Hamiltonian (for $N < \infty$ and $|\Lambda| = N$), which is initially defined on the 2^N -dimensional Hilbert space $\mathcal{H}_N = \bigotimes_{n=1}^N \mathbb{C}^2$, must lie in the range $\text{ran}(S_N)$ of the appropriate symmetrizer S_N on \mathcal{H}_N . Explicitly,

$$S_N(v) = \frac{1}{N!} \sum_{\sigma \in S_n} L_{\sigma}(v), \quad (1.9)$$

with v is a vector in the N -fold tensor product and L_{σ} is given by permuting the factors of v , i.e. $v_1 \otimes \cdots \otimes v_n \mapsto v_{\sigma(1)} \otimes \cdots \otimes v_{\sigma(n)}$. Its range is $(N+1)$ -dimensional, and we show that the quantum Curie–Weiss Hamiltonian restricted to $\text{ran}(S_N)$ becomes a *tridiagonal* $(N+1) \times (N+1)$ matrix. Even for large N , this matrix is easy to diagonalize numerically. Using this tridiagonal structure, in §3 we show that as $N \rightarrow \infty$, our restricted Curie–Weiss Hamiltonian (rescaled by a factor $1/N$) increasingly well approximates a $1d$ Schrödinger operator with a symmetric double well potential defined on the interval $[0, 1]$, in which $\hbar = 1/N$. In §4 we use these ideas to find the counterpart of the “flea” perturbation for the Curie–Weiss model, which, analogously to the double well, localizes the ground state of the perturbed Hamiltonian (where “localization” now refers to spin configuration space rather than real space, of course). We close the main body of the paper with a discussion and outlook, stating some open problems and suggestions for further research. This is followed by an appendix on the Perron–Frobenius Theorem, which plays a central role in our work, and another appendix introducing the discretization techniques we use to non-specialists.

2 Reduction of the Curie–Weiss Hamiltonian

Since the spatial dimension is irrelevant, we may as well consider the Curie–Weiss Hamiltonian (1.5) in $d = 1$, so that we may simply write $|\Lambda| = N$, and, with $h_N \equiv h_N^{\text{CW}}$,

$$h_N = -\frac{1}{2}N^{-1} \sum_{x,y=1}^N \sigma_3(x)\sigma_3(y) - B \sum_{x=1}^N \sigma_1(x). \quad (2.1)$$

It seems folklore that the Perron-Frobenius theorem yields uniqueness of the ground state $\psi_N^{(0)}$ of h_N for any $N < \infty$ and $B \neq 0$, but for completeness we provide the details in Appendix A. It follows that $\psi_N^{(0)}$ is \mathbb{Z}_2 -invariant (see the Introduction), so that there is no SSB for any finite N .

2.1 Tridiagonal form

Let S_N be the standard symmetrizer (1.9) on the Hilbert space $\mathcal{H}_N = \bigotimes_{n=1}^N \mathbb{C}^2$ on which h_N acts, so that S_N projects onto the subspace $\text{ran}(S_N) = \text{Sym}^N(\mathbb{C}^2)$ of totally symmetrized tensors. An orthonormal basis for $\text{Sym}^N(\mathbb{C}^2)$ is given by the vectors $\{|n_+, n_-\rangle \mid n_+ = 0, \dots, N, n_+ + n_- = N\}$, where $|n_+, n_-\rangle$ is the totally symmetrized unit vector in $\bigotimes_{n=1}^N \mathbb{C}^2$, with n_+ spins up and $n_- = N - n_+$ spins down. It follows that this space is $(N + 1)$ -dimensional. Since h_N commutes with S_N , in view of its uniqueness the ground state $\psi_N^{(0)}$ of h_N must also be invariant under S_N . Hence we may expand $\psi_N^{(0)}$ according to

$$\psi_N^{(0)} = \sum_{n_+=0}^N c(n_+/N) |n_+, n_-\rangle, \quad (2.2)$$

where we conveniently introduce a function $c : \{0, 1/N, 2/N, \dots, (N - 1)/N, 1\} \rightarrow [0, 1]$ that satisfies $c(n_+/N) = c(n_-/N)$ as well as $\sum_{n_+=0}^N c^2(n_+/N) = 1$.

Theorem 2.1. *In the basis $\{|n_+\rangle\} \equiv \{|n_+, N - n_+\rangle\}$, the operator (2.1) is an $(N + 1) \times (N + 1)$ tridiagonal matrix:*

$$-\frac{1}{2N}(2n_+ - N)^2 \text{ on the diagonal}; \quad (2.3)$$

$$-B\sqrt{(N - n_+)(n_+ + 1)} \text{ on the upper diagonal}; \quad (2.4)$$

$$-B\sqrt{(N - n_+ + 1)n_+} \text{ on the lower diagonal}. \quad (2.5)$$

Proof. Given two arbitrary vectors $|n_+\rangle$ and $|n'_+\rangle$, we have to compute the expression

$$\langle n_+ | h_N^{\text{CW}} | n'_+ \rangle, \quad (n_+, n'_+ = 0, \dots, N); \quad (2.6)$$

where we have used the bra-ket notation in the above expression. By linearity, we may compute this for the operators

$$\begin{aligned} h_N^{(1)} &= \sum_{x,y=1}^N \sigma_3(x)\sigma_3(y) = \sum_{x=1}^N \sigma_3(x) \cdot \sum_{y=1}^N \sigma_3(y), \quad \text{and} \\ h_N^{(2)} &= \sum_{x=1}^N \sigma_1(x) \end{aligned} \quad (2.7)$$

separately. In order to compute (2.6), we need to know how σ_3 and σ_1 act on the vectors $|n_+\rangle$. Consider therefore the standard basis $\{e_1, e_2\}$ for \mathbb{C}^2 over \mathbb{C} . Then $\{e_{n_1} \otimes \dots \otimes e_{n_N}\}_{n_1=1, \dots, n_N=1}^2$ is the standard basis for $\bigotimes_{n=1}^N \mathbb{C}^2$. Note that the spin-Pauli matrix σ_3 maps e_1 to e_1 and e_2 to $-e_2$, whereas σ_1 maps e_1 to e_2 and e_2 to e_1 . Note that $\sigma_3(x) = 1 \otimes \dots \otimes 1 \otimes \sigma_3 \otimes 1 \dots \otimes 1$, where σ_3 acts on the x^{th} position and similarly for $\sigma_1(x)$. It follows for all $x, y \in \{1, \dots, N\}$ that

$$\begin{aligned} \sigma_3(x)(e_{n_1} \otimes \dots \otimes e_{n_N}) &= \\ 1(e_{n_1}) \otimes \dots \otimes 1(e_{n_{x-1}}) \otimes \sigma_3(e_{n_x}) \otimes 1(e_{n_{x+1}}) \otimes \dots \otimes 1(e_{n_N}) &= \\ \begin{cases} +(e_{n_1} \otimes \dots \otimes e_{n_N}), & \text{if } e_{n_x} = \begin{pmatrix} 1 \\ 0 \end{pmatrix} \\ -(e_{n_1} \otimes \dots \otimes e_{n_N}), & \text{if } e_{n_x} = \begin{pmatrix} 0 \\ 1 \end{pmatrix}. \end{cases} \end{aligned} \quad (2.8)$$

We have $\sigma_3(y)\sigma_3(x)(e_{n_1} \otimes \dots \otimes e_{n_N}) = \pm(e_{n_1} \otimes \dots \otimes e_{n_N})$, where the minus sign appears only if $e_{n_x} \neq e_{n_y}$. We conclude that the standard basis for the N -fold tensor product is a set of eigenvectors for $\sigma_3(y)\sigma_3(x)$ with eigenvalues ± 1 . Thus we know that $\sum_{x,y} \sigma_3(x)\sigma_3(y)$ is a diagonal matrix with respect to this standard basis. Note that $|n_+\rangle$ is a (normalized) sum of permutations of such basis vectors, with n_+ times the vector e_1 and $N - n_+$ times the vector e_2 . Since $\sum_{x,y} \sigma_3(y)\sigma_3(x)$ acts diagonally on any of these vectors, and it is also permutation invariant, it follows that in the inner product any vector with itself yields the same contribution, namely

$$\langle e_1 \otimes \dots \otimes e_1 \otimes e_2 \otimes \dots \otimes e_2 | \sum_{x,y} \sigma_3(y)\sigma_3(x) | e_1 \otimes \dots \otimes e_1 \otimes e_2 \otimes \dots \otimes e_2 \rangle, \quad (2.9)$$

where e_1 occurs n_+ times and e_2 occurs $N - n_+$ times. The above expression equals

$$(n_+ - (N - n_+))^2 = (2n_+ - N)^2,$$

since there are $2n_+(N - n_+)$ minus signs and hence $N^2 - 2n_+(N - n_+) = n_+^2 + (N - n_+)^2$ plus signs, so that in total the correct value is indeed given by

$$n_+^2 + (N - n_+)^2 - 2n_+(N - n_+) = (2n_+ - N)^2. \quad (2.10)$$

This shows that the contribution to the diagonal is given by (2.3).

In order to compute the off-diagonal contribution (2.6) with (2.7), we use an explicit expression for the symmetric basis vector $|n_+\rangle$. Using (1.9), it is not difficult to show that

$$|n_+\rangle = \frac{1}{\sqrt{\binom{N}{n_+}}} \sum_{l=1}^{\binom{N}{n_+}} \beta_{n_+,l}, \quad (2.11)$$

where the subindex l in $\beta_{n_+,l}$ labels the possible permutations of the factors in the basis vector $\beta_{n_+,l}$. Since there are $\binom{N}{n_+}$ such permutations, the subindex indeed goes from 1 to $\binom{N}{n_+}$. We fix N and n_+ , and put

$$\begin{aligned} W_{n_+}^1 &= \{y \in \{1, \dots, N\} | \beta_{n_+} \text{ has } e_1 \text{ on position } y\}, \quad \text{and} \\ W_{n_+}^2 &= \{y \in \{1, \dots, N\} | \beta_{n_+} \text{ has } e_2 \text{ on position } y\}. \end{aligned} \quad (2.12)$$

Then

$$\#W_{n_+}^1 + \#W_{n_+}^2 = n_+ + (N - n_+) = n_+ + n_- = N. \quad (2.13)$$

Both sets are clearly disjoint. Then we compute

$$\begin{aligned} & \frac{1}{\sqrt{\binom{N}{n_+}}} \frac{1}{\sqrt{\binom{N}{n'_+}}} \sum_{l=1}^{\binom{N}{n_+}} \sum_{k=1}^{\binom{N}{n'_+}} \langle \beta_{n_+,l} | h_N^{(2)} | \beta_{n'_+,k} \rangle = \\ & \frac{1}{\sqrt{\binom{N}{n_+}}} \frac{1}{\sqrt{\binom{N}{n'_+}}} \sum_{l=1}^{\binom{N}{n_+}} \sum_{k=1}^{\binom{N}{n'_+}} \langle \beta_{n_+,l} | \sum_{x=1}^N \sigma_1(x) | \beta_{n'_+,k} \rangle = \\ & \frac{1}{\sqrt{\binom{N}{n_+}}} \frac{1}{\sqrt{\binom{N}{n'_+}}} \sum_{l=1}^{\binom{N}{n_+}} \sum_{k=1}^{\binom{N}{n'_+}} \langle \beta_{n_+,l} | \left(\sum_{x \in W_{n_+}^1} + \sum_{x \in W_{n_+}^2} \sigma_1(x) \right) | \beta_{n'_+,k} \rangle = \\ & \frac{1}{\sqrt{\binom{N}{n_+}}} \frac{1}{\sqrt{\binom{N}{n'_+}}} \left(\binom{N}{n_+} (N - n_+) \langle \beta_{n_+,l} | \beta_{n'_+ - 1, k} \rangle + \binom{N}{N - n_+} n_+ \langle \beta_{n_+,l} | \beta_{n'_+ + 1, k} \rangle \right) = \\ & \sqrt{(N - n_+)(n_+ + 1)} \delta_{n_+, n'_+ - 1} + \sqrt{n_+(N - n_+ + 1)} \delta_{n_+, n'_+ + 1}. \end{aligned} \quad (2.14)$$

We used the fact that the vectors $\beta_{n'_+,l}$ are orthonormal, that

$$\frac{1}{\sqrt{\binom{N}{n_+}}} \frac{1}{\sqrt{\binom{N}{n'_+}}} \binom{N}{n_+} (N - n_+) = \sqrt{(N - n_+)(n_+ + 1)}, \quad (2.15)$$

with $n'_+ - 1 = n_+$, and that

$$\frac{1}{\sqrt{\binom{N}{n_+}}} \frac{1}{\sqrt{\binom{N}{n'_+}}} \binom{N}{N - n_+} n_+ = \sqrt{n_+(N - n_+ + 1)}, \quad (2.16)$$

with $n'_+ + 1 = n_+$. Hence the matrix entries of $h_N^{(2)}$ written with respect to the symmetric basis vectors $|n_+, N - n_+\rangle$, are given by $\sqrt{(N - n_+)(n_+ + 1)}$ on the upper diagonal and by $\sqrt{n_+(N - n_+ + 1)}$ on the lower diagonal.

We conclude that the Hamiltonian with respect to this basis is a tridiagonal matrix with the desired entries (see also van de Ven, 2018, §3.1). \square

2.2 Numerical simulations

In the next section we will argue that for $0 < B < 1$ the above $(N + 1)$ -dimensional matrix, which we denote by J_{N+1} , can be linked to a Schrödinger operator with a symmetric double well on $L^2([0, 1])$, for N sufficiently large. Since for a sufficiently high and broad enough potential barrier the ground state of such a Schrödinger operator is approximately given by two Gaussians, each of them located in one of the wells of the potential, we might expect the

same result for J_{N+1} . In fact, the first two eigenfunctions of this Schrödinger operator are approximately given by

$$\psi^{(0)} \cong \frac{T_a(\varphi_0) + T_{-a}(\varphi_0)}{\sqrt{2}}, \quad \psi^{(1)} \cong \frac{T_a(\varphi_0) - T_{-a}(\varphi_0)}{\sqrt{2}}, \quad (2.17)$$

where $T_{\pm a}$ is the translation operator over distance a (i.e., $(T_{\pm a}\varphi_0)(x) = \varphi_0(x \pm a)$), where $\pm a$ denotes the minima of the potential well. The functions φ_n are the weighted Hermite polynomials given by $\varphi_n(x) = e^{-x^2/2}H_n(x)$, with H_n the Hermite polynomials. We diagonalized the operator J_{N+1} and plotted the first two (discrete) eigenfunctions $\psi_N^{(0)}$ and $\psi_N^{(1)}$. For convenience, we scaled the grid to unity. See Figures 1 and 2. From these two plots, it is quite clear that both eigenvectors of h_N^{CW} are approximately given by (2.17).⁶ In

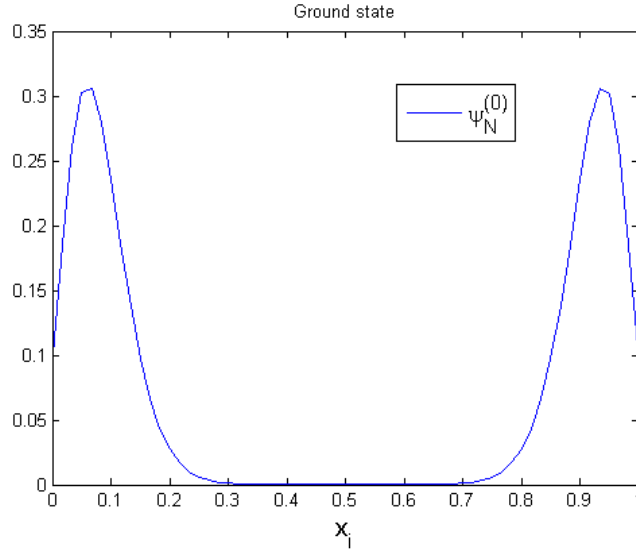


Figure 1: The ground state eigenfunction of h_N^{CW} , computed from the tridiagonal matrix J_{N+1} for $N = 60$, $J = 1$ and $B = 1/2$. The grid points on the horizontal axis are labeled by $x_i = i/N$ for $i = 0, \dots, N$.

the next section, we will see that for $0 < B < 1$ each of the two peaks of the ground state eigenvector of the N -dependent Curie–Weiss Hamiltonian is indeed located in one of the wells of some symmetric potential. However, due to numerical degeneracy of the ground state $\psi_N^{(0)}$ and first excited state $\psi_N^{(1)}$ for about $N \geq 80$ (see the figure below), these two states will form a linear combination, even though mathematically the ground state is unique for any finite N .⁷ This is also exactly what we observe for the values $N \geq 80$: plotting the ground state and the first excited state of h_N^{CW} ($B = 1/2$ and $J = 1$) gives a Gaussian shaped curve,

⁶However, one has to beware of the following fact: since we do not know if the first excited state is unique, it might happen that it does not lie in $\text{Sym}^N(\mathbb{C}^2)$. As a result, it could happen that the first excited state computed from the tridiagonal matrix J_{N+1} , is not the same as the one from the original Hamiltonian h_N^{CW} , in which case Figure 2 would be misleading. Fortunately, we have shown numerically up to $N = 12$, that the first excited state of h_N^{CW} represented as a matrix on the space \mathbb{C}^{2^N} is indeed the same as the one corresponding to the tridiagonal matrix J_{N+1} .

⁷This numerical degeneracy is an observation from our simulations for $N \geq 80$.

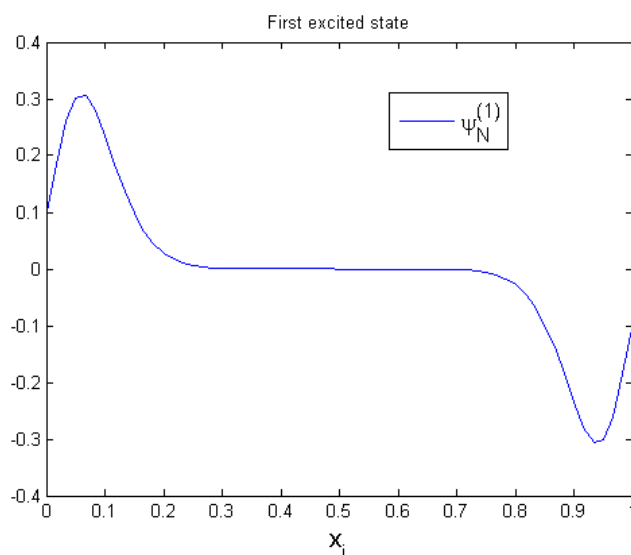


Figure 2: The first excited state of h_N^{CW} , computed from the tridiagonal matrix J_{N+1} for $N = 60$, $J = 1$ and $B = 1/2$. The grid points on the horizontal axis are indicated by $x_i = i/N$ for $i = 0, \dots, N$.

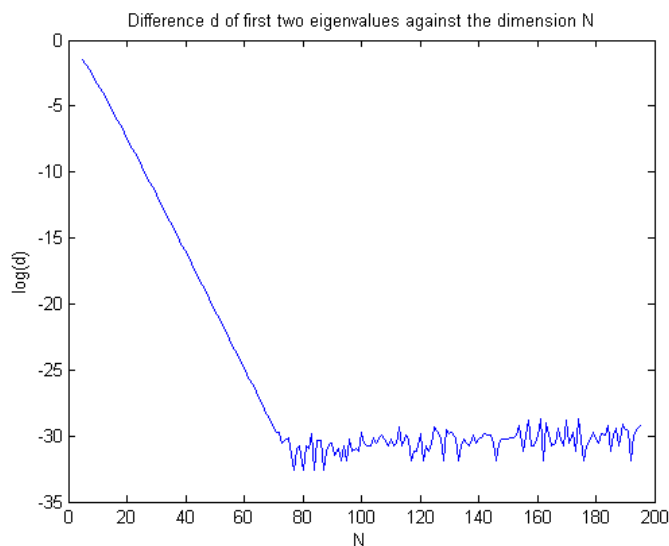


Figure 3: Energy splitting $d = |\epsilon_N^{(0)} - \epsilon_N^{(1)}|$ between the first two eigenvalues $\epsilon_N^{(0)}$ and $\epsilon_N^{(1)}$ of the tridiagonal matrix J_{N+1} , for different values of N on a log scale. From about $N = 80$ onwards, the energy splitting is in the order of the maximum achievable accuracy of the eigenvalues, so that the first two eigenvalues become numerically degenerate.

each located in one of the wells.⁸ Indeed, assuming that $\psi_N^{(1)}$ is in $\text{Sym}^N(\mathbb{C}^2)$, then for these relative large values of N , the new (numerical) degenerate ground state eigenvector is given

⁸We checked this numerically, but omitted the plots.

by the functions

$$\chi_+ = \frac{\psi_N^{(0)} + \psi_N^{(1)}}{\sqrt{2}}; \quad \chi_- = \frac{\psi_N^{(0)} - \psi_N^{(1)}}{\sqrt{2}}. \quad (2.18)$$

Using this result and equation (2.17), it follows by a simple calculation that

$$\chi_+ \cong T_a \varphi_0; \quad \chi_- \cong T_{-a} \varphi_0. \quad (2.19)$$

Of course, the functions $\varphi_n(x)$ now have to be understood as functions on a discrete grid. For $N = 60 < 80$, we have seen in Figure 1 above that the ground state is doubly peaked and therefore given by $\psi_N^{(0)}$, rather than χ_+ . This makes sense, since the energy levels are not yet degenerate even for the computer.

3 From Curie–Weiss to a discretized Schrödinger operator

Discretization is the process of approximating the derivatives in (partial) differential equations by linear combinations of function values f at so-called *grid points*. The idea is to discretize the domain, with N of such grid points, collectively called a *grid*. We give an example in one dimension.

$$\Omega = [0, X], \quad f_i \approx f(x_i), \quad (i = 0, \dots, N), \quad (3.1)$$

with grid points $x_i = i\Delta$ and grid size $\Delta = X/N$. The symbol Δ is called the *grid spacing*. Note this the grid spacing is chosen to be constant or uniform in this specific example. For the first order derivatives we have

$$\frac{\partial f}{\partial x}(\bar{x}) = \lim_{\Delta x \rightarrow 0} \frac{f(\bar{x} + \Delta x) - f(\bar{x})}{\Delta x} = \lim_{\Delta x \rightarrow 0} \frac{f(\bar{x}) - f(\bar{x} - \Delta x)}{\Delta x} = \lim_{\Delta x \rightarrow 0} \frac{f(\bar{x} + \Delta x) - f(\bar{x} - \Delta x)}{2\Delta x}. \quad (3.2)$$

These derivatives are approximated with *finite differences*. There are basically three types of such approximations:

$$\begin{aligned} \left(\frac{\partial f}{\partial x}\right)_i &\approx \frac{f_{i+1} - f_i}{\Delta x} \quad (\text{forward difference}) \\ \left(\frac{\partial f}{\partial x}\right)_i &\approx \frac{f_i - f_{i-1}}{\Delta x} \quad (\text{backward difference}) \\ \left(\frac{\partial f}{\partial x}\right)_i &\approx \frac{f_{i+1} - f_{i-1}}{2\Delta x} \quad (\text{central difference}). \end{aligned} \quad (3.3)$$

Since it is more accurate in our case, will focus on the central difference approximation method and apply this to the second order differential operator d^2/dx^2 .

3.1 Locally uniform discretization

In the example above, the grid spacing was chosen to be uniform. Now reconsider this example on the domain $\Omega = [0, 1]$ with uniform grid spacing $\Delta = 1/N$. The second order derivative operator is approximately given by

$$f_i'' \approx \frac{f_{i-1} - 2f_i + f_{i+1}}{\Delta^2} + O(\Delta^2) \quad (i = 1, \dots, N). \quad (3.4)$$

By throwing away the error term $O(\Delta^2)$ in the above equation, it follows that we can approximate the second derivative operator in matrix form

$$\frac{1}{\Delta^2} \begin{pmatrix} -2 & 1 & & & \\ 1 & -2 & 1 & & 0 \\ & \ddots & \ddots & \ddots & \\ 0 & 1 & -2 & 1 & \\ & & & 1 & -2 \end{pmatrix}. \quad (3.5)$$

This matrix is the standard discretization of the second order derivative on a uniform grid consisting of N points of length $\Delta \cdot N$, with uniform grid spacing Δ . In this specific case, we have $\Delta = 1/N$. We denote this matrix also by $\frac{1}{\Delta^2}[\cdots 1 -2 1 \cdots]_N$.

Suppose now that we are given a symmetric tridiagonal matrix A of dimension N with constant off- and diagonal elements:

$$A = \begin{pmatrix} b & a & & & \\ a & b & a & & 0 \\ & \ddots & \ddots & \ddots & \\ 0 & a & b & a & \\ & & & a & b \end{pmatrix}. \quad (3.6)$$

We are going to extract a kinetic and a potential energy from this matrix. We write

$$A = a[\cdots 1 \frac{b}{a} 1 \cdots]_N = a[\cdots 1 -2 1 \cdots]_N + \text{diag}(b + 2a), \quad (3.7)$$

where the latter matrix is a diagonal matrix with the element $b + 2a$ on the diagonal. It follows that

$$A = T + V, \quad (3.8)$$

for $T = a[\cdots 1 -2 1 \cdots]_N$, and $V = \text{diag}(b + 2a)$. In view of the above, the matrix T corresponds to a second order differential operator. This matrix plays the role of (3.5), but with uniform grid spacing $1/\sqrt{a}$ on the grid of length N/\sqrt{a} . Since the matrix V is diagonal, it can be seen as a multiplication operator. Therefore, given such a symmetric tridiagonal matrix A , we can derive an operator that is the sum of a discretization of a second order differential operator and a multiplication operator. The latter operator is identified with the potential energy of the system. Hence, we can identify A with a discretization of a Schrödinger operator.⁹

The next step is to understand what happens in the case where we are given a symmetric tridiagonal matrix with non-constant off- and on-diagonal elements. This is important as we will see, since the Curie–Weiss Hamiltonian, written with respect to the canonical symmetric basis for the subspace $\text{Sym}^N(\mathbb{C}^2)$ of $\mathbb{C}^{2^N} \simeq \bigotimes_{n=1}^N \mathbb{C}^2$, is precisely an example of such matrix. The question we ask ourselves is if we can link such a matrix to a discretization of a Schrödinger operator as well.

Let us first review the second order differential operator $\frac{d^2}{dx^2}$. In most central finite difference applications *non-uniform grids* are employed, allowing the grid to be more refined in regions

⁹Strictly speaking we have to put a minus sign in front of T , as the kinetic energy is defined as $-\frac{d^2}{dx^2}$.

where strong gradients are expected. In that case the grid points x_i ($i = 1, \dots, N$) are not uniformly distributed over the domain. We define $h_j = x_{j+1} - x_j$ ($i = 1, \dots, N$). Then the length of the domain of discretization is given by $\sum_{j=1}^N h_j$. In the central difference approximation, the second order derivative is given by (see Appendix B):

$$f_j'' = \frac{2f_{j-1}}{h_{j-1}(h_{j-1} + h_j)} - \frac{2f_j}{h_{j-1}h_j} + \frac{2f_{j+1}}{h_j(h_{j-1} + h_j)} + O(h^2). \quad (3.9)$$

Now suppose we are given a symmetric tridiagonal matrix B with non-constant off- and on-diagonal elements. As for the uniform case, the question we asked ourselves was whether we can link this matrix to a discretization of a Schrödinger operator. We will see below that the off-diagonal elements must have the form c, d, c, d, c, d, \dots , in order to link the matrix B to a discretization of a second order derivative operator. Note that we cannot easily apply the same procedure as in the uniform case, since the matrix entries are not constant. Therefore, we identify the matrix B with (3.9), where we throw away the error term $O(h^2)$ again. It follows that

$$B_{j,j+1} = \frac{2}{h_j(h_{j-1} + h_j)}, \quad (3.10)$$

$$B_{j,j} = \frac{-2}{h_{j-1}h_j}, \quad (3.11)$$

$$B_{j,j-1} = \frac{2}{h_{j-1}(h_{j-1} + h_j)}. \quad (3.12)$$

We can compute the non-uniform grid spacing h_j as follows. We put

$$\rho_j = \frac{B_{j,j+1}}{B_{j,j-1}} = \frac{h_{j-1}}{h_j}. \quad (3.13)$$

Combined with the above three equations, we derive from this expression that

$$h_j^2 = \frac{2}{B_{j,j+1}(1 + \rho_j)}. \quad (3.14)$$

From (3.12), we also find

$$h_{j-1}^2 = \frac{2}{B_{j,j-1}(1/\rho_j + 1)}. \quad (3.15)$$

From $h_{(j-2)+1} = h_{j-1}$, it now follows that

$$\rho_{j-1} = \frac{1}{\rho_j}, \quad \text{or equivalently,} \quad (3.16)$$

$$B_{j+1,j} = B_{j-1,j-2}, \quad \text{and} \quad B_{j,j-1} = B_{j-2,j-3}, \quad (3.17)$$

where we used the fact that the matrix is symmetric. This means that the off-diagonal matrix entries of B must have the form c, d, c, d, c, d, \dots . If this is the case, then indeed we can identify B with a discretization of a second order differential operator. This is clearly true for (3.6), since the off-diagonal entries are all equal. Moreover, the potential energy is then obtained by subtracting (3.11) from the diagonal of B . The result is that such a tridiagonal

matrix with this symmetry of the off-diagonal elements can also be written as a sum of a kinetic and a potential energy operator and hence corresponds to a discrete analog of a $1d$ Schrödinger operator in a potential well.

Consider our tridiagonal matrix J_{N+1} . This matrix is tridiagonal with non-constant off- and diagonal entries. In view of the above, we therefore apply the non-uniform discretization process in order to identify this matrix with a discretization of a second order derivative operator and a multiplication operator. At first sight, for any finite $N > 0$, the matrix J_{N+1} does not have off-diagonal elements of the form c, d, c, d, c, d, \dots , let alone c, c, c, c, \dots . However, we argue in this subsection that the scaled matrix J_{N+1}/N has approximately constant off-diagonal entries on a length scale of $O(\sqrt{N})$ for N large enough. This means that, at least on these length scales and N large enough, the grid spacing becomes approximately uniform. It turns out (details given in §3.2 and §3.3) that the matrix J_{N+1}/N locally approximates some discretization matrix à la (3.6) corresponding to a Schrödinger operator describing a particle in a symmetric double well potential, for large, but finite N .¹⁰

We write $T = J_{N+1}$. Then as before, consider the ratios:

$$\rho_j = \frac{h_{j-1}}{h_j} = \frac{T_{j+1}}{T_{j-1}} \quad (j = 1, \dots, N), \quad (3.18)$$

with non-uniform grid spacing h_j and h_{j-1} . We divide the original tridiagonal matrix J_{N+1} by N for scaling. Thus, we consider J_{N+1}/N . If we then compute the distances h_j , we see that they are almost all of $O(1)$, except at the boundaries. Since we then have approximately N distances of each order 1, we will see later that the corresponding Schrödinger operator analog of the matrix J_{N+1}/N will be an operator on a domain of length of order N . More precisely, the domain is $[0, \sqrt{8N}]$, see the explanation below (3.45).

First, we compute the ratios ρ_j :

$$\rho_j = \frac{T_{j+1}}{T_{j-1}} = \frac{\sqrt{(N-j)(j+1)}}{\sqrt{(N-j+1)j}} = \sqrt{\frac{N-j}{N-j+1}} \sqrt{\frac{j+1}{j}} = \sqrt{\frac{1}{1 + \frac{1}{N-j}}} \sqrt{1 + \frac{1}{j}}. \quad (3.19)$$

Use the following approximations

$$\sqrt{1 + \frac{1}{j}} \approx 1 + O\left(\frac{1}{2j}\right) = 1 + O(1/j) \quad \text{and} \quad (3.20)$$

$$\sqrt{\frac{1}{1 + 1/(N-j)}} \approx 1 - O\left(\frac{1}{2(N-j)}\right) = 1 + O\left(\frac{1}{N-j}\right), \quad (3.21)$$

and observe that for $j \gg 1$ and $N - j \gg 1$, we have

$$\sqrt{1 + \frac{1}{j}} \approx O(1) \quad \text{and} \quad (3.22)$$

$$\sqrt{\frac{1}{1 + 1/(N-j)}} \approx O(1), \quad (3.23)$$

¹⁰In order to show this, we see in this subsection that in the limit $N \rightarrow \infty$ we have uniform discretization on an interval of length $O(\sqrt{N})$. Making N large enough, this discretization will be already approximately uniform and thus we have an approximate kinetic energy with emergent Schrödinger operator.

Moreover, we see that the ratio satisfies

$$\rho_j \approx 1 + O(1/j) + O\left(\frac{1}{N-j}\right), \quad (3.24)$$

using the fact that the big-O notation respects the product, that $O(\frac{1}{j} \frac{1}{N-j}) \leq O(1/j)$, and also $O(\frac{1}{j} \frac{1}{N-j}) \leq O(\frac{1}{N-j})$.

In the next subsection, we will see from numerical simulations that to a good approximation the ground state eigenfunction is a double peaked Gaussian with maxima centered in the minima of some double well potential that we are going to determine. This potential occurs in a discrete Schrödinger operator analog of the matrix J_{N+1}/N for N large, i.e., in the semiclassical limit. By these calculations (see §3.2), it follows that when we map the double well on the unit interval the two minima of the symmetric double well are given by

$$\frac{1}{2} \pm \frac{1}{4}\sqrt{3}. \quad (3.25)$$

On the interval $[0, 1]$ these minima are of order 1, and when we consider the potential on the original domain $[0, \sqrt{8}N]$ of order N , the minima are of order

$$\left(\frac{1}{2} \pm \frac{1}{4}\sqrt{3}\right)N = O(N). \quad (3.26)$$

Furthermore, we showed by numerical simulations (Figure 4 below) that the width σ of each Gaussian-shaped¹¹ ground state of J_{N+1} located at one of minima of the potential is of order \sqrt{N} , and hence that each peak rapidly decays to zero, so that the ground state eigenfunction is approximately zero at both boundaries. In particular, the size of the domain where the peak is non-zero is of order \sqrt{N} , as we clearly observe from the figure. This is an approximation, since we neglect the (relatively small) function values of the Gaussian that are more than $O(\sqrt{N})$ away from the central maximum. However, this approximation is highly accurate, as the Gaussian decays to zero exponentially. This observation is extremely important, as we will now see.

Let us first focus on the left-located Gaussian. For a point $x_j = j/N$ in the domain of order N , clearly $j \in O(N)$. Therefore, for N large enough,

$$\rho_j = 1 + O(1/N), \quad (3.27)$$

since for these values of $j < N - j$ we have $O(\frac{1}{N-j}) \leq O(1/j)$. For the right-located peak, we have $N - j < j$, so that in this case $O(1/j) \leq O(\frac{1}{N-j})$, and we find

$$\rho_j = 1 + O\left(\frac{1}{N-j}\right). \quad (3.28)$$

We will now show that, in the present context where we work on a domain of order N (i.e. $[0, \sqrt{8}N]$), we indeed have uniform discretization on an interval of length of order \sqrt{N} .

We start with the peak on the left. Since the error per step that we make equals ρ_j , it follows that the error on the interval of length of order σ equals $\rho_j^\sigma \approx (1 + \frac{1}{N})^\sigma$ for $j < N - j$

¹¹We mean that if we plot the discrete points and draw a line through these points, then the corresponding graph has the shape of a Gaussian.

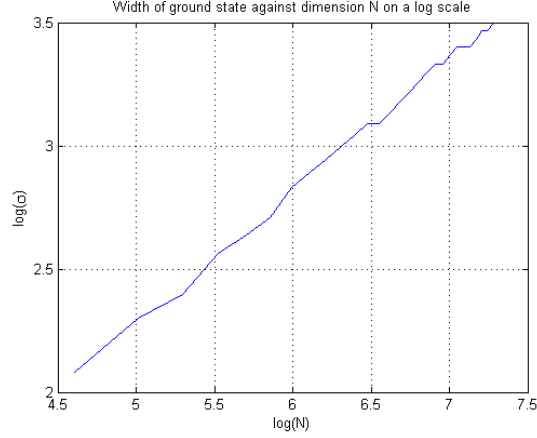


Figure 4: The width at half height of the ground state eigenvector of J_{N+1} ($B = 1/2$ and $J = 1$) against N , for $N = 100 : 50 : 1500$ on a log scale. The slope of the line is about 0.5, which means that the width σ goes like \sqrt{N} .

and N large. Denoting the off-diagonal element corresponding to the minimum x_{j_0} of the potential well by T_{j_0} , for the off-diagonal elements within a range of order σ , we derive the next estimate:

$$|T_{j_0} - T_{j_0+\sigma}| \approx |T_{j_0} - O\left(1 + \frac{1}{N}\right)^\sigma T_{j_0}| = T_{j_0} \left|1 - O\left(1 + \frac{1}{N}\right)^\sigma\right| \leq C \frac{\sigma}{N}, \quad (3.29)$$

where we used the inequality $(1 + 1/N)^\sigma \leq 1 + C \frac{\sigma}{N}$ as well as the fact that T_{j_0} is of order 1. Here, $C > 1$ is a constant independent of N . Since the left peak of the Gaussian eigenfunction is approximately non-zero within an interval of length of order \sqrt{N} , we apply the above estimate to $\sigma \approx \sqrt{N}$. We see immediately that $|T_{j_0} - T_{j_0+\sigma}|$ goes to zero. Therefore, on an interval of length of order \sqrt{N} centered around the left minimum x_{j_0} of the potential, the off-diagonal elements coincide in the limit $N \rightarrow \infty$. This means that the grid spacing becomes constant and hence that we have locally uniform discretization of the domain. By symmetry, the same is true for the peak located on the right of the well. We conclude that for large N the tridiagonal matrix locally behaves like a kinetic energy, and therefore like a discretized Schrödinger operator. All this will be explained in more detail in the next two subsections. Furthermore, note that this result is independent of the location of the interval of order \sqrt{N} .¹² However, since we observe numerically that the Gaussian-shaped ground state located in the domain of order N attains its maxima at $N(\frac{1}{2} \pm \frac{1}{4}\sqrt{3})$ and exponentially decays to zero, the only interval that might play a role is the one centered around these maxima. We return to this point in the next subsection.

3.2 Link with a discrete Schrödinger operator

Our aim is to show that for N large enough, the matrix J_{N+1}/N obtained from the Curie–Weiss Hamiltonian by reduction (see §2) locally approximates a discretization matrix corresponding to a Schrödinger operator describing a particle moving in a symmetric double well. This means that there exists a sub-block of J_{N+1}/N that has a form approximately given

¹²This result only holds for those intervals which are away from both boundaries.

by the sum of $-\frac{1}{h^2}[\cdots 1 - 2 \ 1 \cdots]_{N+1}$ (for some h to be determined) and a diagonal matrix playing the role of a potential. We started with the symmetric tridiagonal matrix J_{N+1}/N with non-constant entries. In order to link this matrix to a second derivative and a multiplication operator, we needed to apply the non-uniform discretization procedure. The off-diagonal matrix entries of J_{N+1}/N do not have the form c, d, c, d, c, d, \dots , for any finite N . Therefore, we could not immediately identify this matrix with a second order derivative operator. However, we have seen that in the limit $N \rightarrow \infty$, we do have uniform discretization on some interval of a length scale of $O(\sqrt{N})$ of the total domain of discretization. Consequently, for sufficiently large N this discretization becomes approximately uniform on this length scale. From this, we are now going to extract a matrix of the form (3.6) corresponding to a Schrödinger operator on $L^2([0, 1])$. Let us first state the main results of this subsection and of subsection §3.3. We consider the $(N \times N)$ -matrix \tilde{H}_N , defined as

$$\tilde{H}_N = \tilde{T}_N + \tilde{V}_N, \quad (3.30)$$

where

$$\tilde{T}_N = -\frac{1}{8}[\cdots 1 - 2 \ 1 \cdots]_N \quad (3.31)$$

and \tilde{V}_N is a diagonal matrix (and hence a multiplication operator, as in the continuum) given by

$$\tilde{V}_N = -\frac{1}{2}\left(\frac{2j}{N} - 1\right)^2 - B\left(\sqrt{\left(1 - \frac{j}{N}\right)\left(\frac{j}{N} + \frac{1}{N}\right)} + \sqrt{\left(1 - \frac{j}{N} + \frac{1}{N}\right)\frac{j}{N}}\right), \quad (j = 1, \dots, N). \quad (3.32)$$

We will show that J_{N+1}/N locally approximates \tilde{H}_{N+1} for large N . Recall that this means that the matrix J_{N+1}/N contains a sub-block (of dimension of $O(\sqrt{N})$) that approximates a sub-block of the matrix \tilde{H}_N , when N increases.¹³ We see in this section that to a very good approximation even the spectral properties of both (a priori different) matrices J_{N+1}/N and \tilde{H}_{N+1} coincide, improving with increasing N . In §3.3, we show that the matrix \tilde{H}_N is a discretization of a particular Schrödinger operator \tilde{h}_2 on $L^2([0, 1])$ with the familiar substitution $\tilde{h} = \frac{1}{N}$. This operator is defined as

$$\tilde{h}_2 = -\frac{1}{8N^2} \frac{d^2}{dy^2} + m_{\tilde{V}}. \quad (3.33)$$

The potential \tilde{V} (for $B = 1/2$ and $J = 1$) is then given by the continuous function

$$\tilde{V}(y) = -\frac{1}{2}(2y - 1)^2 - \sqrt{(1 - y)y}, \quad y \in [0, 1]. \quad (3.34)$$

The first step is to show that the matrix \tilde{H}_{N+1} defined by (3.30) can indeed be locally approximated by J_{N+1}/N . As we have seen in the previous subsection, for N large enough,

¹³We have briefly explored alternative mappings of a tridiagonal matrix with non-constant off-diagonal elements onto a discretized 1d Schrödinger operator. One option is to start with the matrix representation of eqs. (3.38)-(3.40) for a non-uniform grid and explicitly symmetrize it. Another option is to use an equally spaced grid, but make the mass position dependent. These approaches raise the question how and under which conditions the spectra of these Schrödinger operators converge to the spectrum of the original matrix. The questions go beyond the scope of the present paper and we do not elaborate on these approaches here.

we locally have an approximate uniform discretization of the domain of discretization, using the fact that some of the off-diagonal elements are approximately constant. This implies that we can identify a sub-block of the matrix J_{N+1}/N with a second-order derivative and hence with a kinetic energy T and a potential V . The latter operator is obtained by subtracting the kinetic energy contribution to the diagonal from the diagonal of the original matrix J_{N+1}/N . Let us first focus on the kinetic energy. We want to identify this sub-block with a kinetic energy operator of the form:

$$T = -\frac{1}{h^2} [\cdot \cdot \cdot 1 \ -2 \ 1 \ \cdot \cdot \cdot]. \quad (3.35)$$

This matrix is the second-order derivative on a grid of length $h \cdot \dim(\text{sub-block})$, where the dimension of this sub-block is approximately equal to \sqrt{N} , as explained in the last part of §3.1. The constant h denotes the uniform grid spacing.¹⁴ This value can be determined using Appendix B. The value of h is fixed by (B.22), i.e.,

$$h_j = \sqrt{-\frac{2}{T_{j,j+1}(1 + \rho_j)}}. \quad (3.36)$$

As we know, for large N , the values h_j are approximately constant on some subset (of order \sqrt{N}) of the domain. This subset was located around the maxima of both Gaussian-shaped ground state peaks. If we then denote the grid spacing at the central maximum of both Gaussians by h_{j_0} , we find numerically that $h_{j_0}^2 \approx 8$, for $N = 5000$.¹⁵ This approximation gets better for increasing N . Moreover, we observe also from numerical calculations that the approximation of the number 8 by h_j^2 becomes better for those values of h_j that belong to the entire subset of $O(\sqrt{N})$, when N gets larger. This reconfirms our previous observation that the subdomain centered around x_{j_0} is uniformly discretized with grid spacing $h = \sqrt{8}$. Hence, we have shown that the matrix J_{N+1}/N contains a sub-block¹⁶ for which the kinetic energy is approximately given by (3.35), for $h = \sqrt{8}$. Since we have seen that locally around the maxima of both Gaussians the kinetic energy contribution to the diagonal approximately equals $2/h^2 \approx 1/4$ (see (3.11)), it follows that the potential V in this sub-block is approximately given by

$$V \approx \text{diag}(J_{N+1}/N) - 1/4. \quad (3.37)$$

Hence, the matrix J_{N+1}/N contains two sub-blocks that can be approximately written as sum of a kinetic energy T and a potential energy V .

The next step in the process of the analysis regarding the matrix \tilde{H}_N is to explain how the potential \tilde{V}_N given by (3.32) is obtained. In order to find this matrix \tilde{V}_N , we again start with J_{N+1}/N . We apply the same procedure as before, namely, we first compute the contribution of the ‘kinetic energy’ \tilde{K}_N to the diagonal of J_{N+1} on the *entire* domain of discretization, using the formula (cf. (3.11))

$$\tilde{K}_N(j, j) = -\frac{2}{\rho_j h_j^2} \quad (j = 1, \dots, N + 1). \quad (3.38)$$

¹⁴Note that this result is in accordance with (3.8) for $a = 1/h^2$, since the corresponding grid spacing is $1/\sqrt{a} = h$.

¹⁵This is a result of the fact that $\rho_j \approx 1$ and $T_{j,j+1} \approx -1/8$, for these values of j .

¹⁶By symmetry of the ground state, there are two subsets of order \sqrt{N} on which the discretization is uniform. As a result, the matrix J_{N+1}/N contains two of such sub-blocks.

We use quotation marks to indicate that \tilde{K}_N is not a kinetic energy, because the discretization is not uniform globally.¹⁷ We just use this as a trick to compute \tilde{V}_N for the matrix \tilde{H}_N . As before, we compute \tilde{V}_N by

$$\tilde{V}_N = \text{diag}(J_{N+1}/N) - \tilde{K}_N(j, j), \quad (j = 1, \dots, N + 1). \quad (3.39)$$

We simplify (3.39) using (3.38), and start with J_{N+1} . Write $\tilde{K}_N(k, j) \equiv \tilde{K}_{k,j}$, $\tilde{V}_N(k, j) \equiv \tilde{V}_{k,j}$ and $J_{N+1}(k, j) \equiv J_{k,j}$. Elaborating formula (3.38) for \tilde{K}_N gives

$$\tilde{K}_{j,j} = -(J_{j,j-1} + J_{j,j+1}), \quad (3.40)$$

where $J_{j,j\pm 1}$ are the off-diagonal entries of the tridiagonal matrix J_{N+1} . Substituting the expressions for $J_{j,j\pm 1}$, shows that the above equation is equal to

$$\tilde{K}_{j,j} = B(\sqrt{(N-j)(j+N)} + \sqrt{(N-j+1)j}). \quad (3.41)$$

It follows that (3.39) reads

$$\tilde{V}_{j,j} = J_{j,j} - (-(J_{j,j-1} + J_{j,j+1})). \quad (3.42)$$

One should mention that the above equation (3.42) approximately equals formula (3.37) for N large enough, since $\tilde{T}_{j,j} \approx \frac{1}{4}$ for those j corresponding to the sub-block on which the discretization is approximately uniform. Substituting the expressions for $J_{j,j}$ and $T_{j,j\pm 1}$ gives

$$\tilde{V}_{j,j} = -\frac{1}{2N}(2j - N)^2 - B(\sqrt{(N-j)(j+1)} + \sqrt{(N-j+1)j}). \quad (3.43)$$

Using the identity $j = \frac{iN}{N}$, the above expression (3.43) for the potential equals

$$\tilde{V}_{j,j} = N \left(-\frac{1}{2} \left(\frac{2j}{N} - 1 \right)^2 - B \left(\sqrt{\left(1 - \frac{j}{N}\right) \left(\frac{j}{N} + \frac{1}{N}\right)} + \sqrt{\left(1 - \frac{j}{N} + \frac{1}{N}\right) \frac{j}{N}} \right) \right). \quad (3.44)$$

Then for J_{N+1}/N , we see that the factor N in front of the above equations disappears. With abuse of notation, we put $\tilde{V}_N \equiv \tilde{V}/N$. Note that \tilde{V}_N is indeed given by (3.32). Finally, using (3.31) for the kinetic energy, we define the $(N \times N)$ -matrix \tilde{H}_N by

$$\tilde{H}_N = \tilde{T}_N + \tilde{V}_N. \quad (3.45)$$

As we will see in §3.3, this is in fact a discretization of the Schrödinger operator (3.33).

We have to be careful with the domain of the matrix J_{N+1}/N . The length of the domain is given by the sum of all distances h_j , where j runs from 0 to N . We computed this length and this approximately gives $2.4N$, for N large enough. Therefore, each point x_j in the domain corresponds to the sum $\sum_{k=1}^j h_k$. In particular, $\sum_{k=1}^n h_k \approx 2.4N$. However, as we have just seen, the operator \tilde{T}_N and hence \tilde{H}_N is defined on a domain of approximate length of $\sqrt{8}N$, which is fortunately the same order $O(N)$ as $2.4N$.

Remark. Consider the Schrödinger operator with a symmetric double well potential, given by (1.1). Recall from §2.2 that for a sufficiently high and broad potential well, the ground state of such a Schrödinger operator is approximately given by two Gaussians, each of them located in one of the wells of the potential. This fact will be useful for the next round of observations.

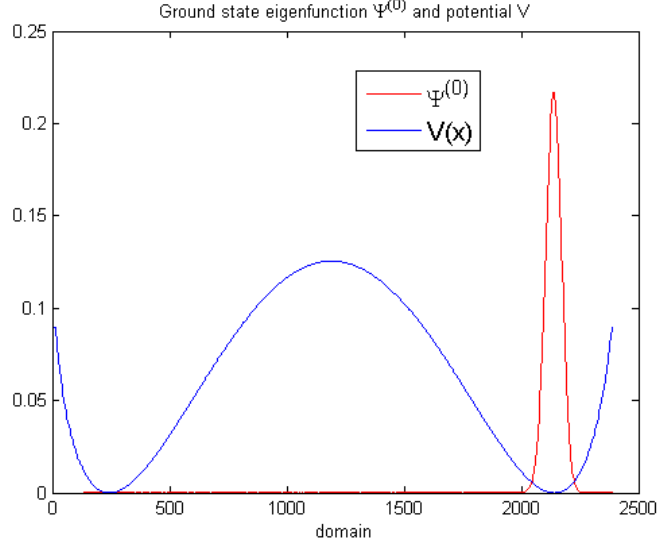


Figure 5: The scaled potential \tilde{V}_N and the ground state eigenfunction corresponding to J_{N+1}/N for $N = 1000$. The potential is shifted so that its minimum is zero. The length of the domain is approximately equal to $2.4N$, as explained above. The parameters $B = 1/2$ and $J = 1$ are still fixed.

We will now see that the Gaussian-shaped ground state of J_{N+1}/N , indeed localizes in both minima of the potential well \tilde{V}_N . To this end, we have made a plot of the scaled potential \tilde{V}_N from equation (3.44) on a domain of length $2.4N$, for $B = 1/2$ and $J = 1$. See Figure 5.

We immediately recognize the shape of a symmetric double well potential. The points in its domain are given by $x_j = \sum_{k=1}^j h_k$ for $j = 0, \dots, N$. Then we diagonalized the matrix J_{N+1}/N and computed the ground state eigenvector. We plot this together with the potential in Figure 5. One should mention that there is only one Gaussian peak visible, not two. As we have seen in §2.2, this must be due to the finite precision of the computer i.e., the first two eigenvalues are already numerically degenerate. Thus the computer picks a linear combination of the first two eigenvectors as ground state (viz. (2.18)), even though we know from the Perron-Frobenius Theorem (Appendix A) that the ground state is always unique for any finite N .¹⁸ We also observe that the maxima of the Gaussian ground state peaks are precisely centered in the minima of these two wells (as should be the case). It is clear from this figure that the ground state is localized in (one of) the minima of the double well.

One might suggest that there would be some critical value of N for which the eigenvalues are not yet degenerate for the computer. We have seen in Figure 3 that this value of N is about $N = 80$. Figure 6 is a similar plot for the ground state for $N = 60$, on a par with Figure 1 in §2.2.

We recognize the well-known doubly peaked Gaussian shape, but now it is localized in both minima of the potential well. This is displayed in Figure 6.

These figures show that there is a convincing relation between the matrix J_{N+1}/N and a

¹⁷This follows from the fact that ρ_j is not approximately equal to one for all $i = 1, \dots, N + 1$.

¹⁸Due to this degeneracy, the computer picks or the symmetric combination χ_+ , or the anti-symmetric combination χ_- , which depends on the algorithm.

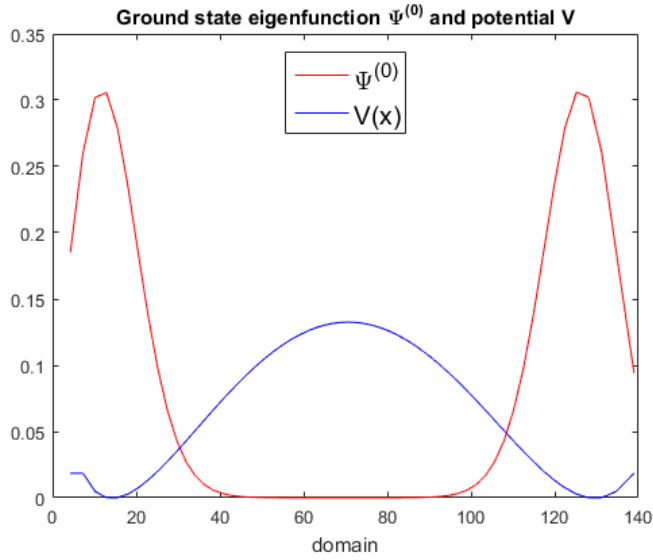


Figure 6: The scaled and shifted potential \tilde{V}_N for $B = 1/2$ and $J = 1$, and the ground state eigenfunction corresponding to J_{N+1}/N for $N = 60$. Also here, the length of the domain is approximately $2.4N$. The ground state (discrete) eigenvector is normalized to 1.

Schrödinger operator describing a particle in a double well. The double well shaped potential is a result of the choice $B = 1/2$. The value of the magnetic field needs to be within $[0, 1)$ in order to get spontaneous symmetry breaking of the ground state in the classical limit $N \rightarrow \infty$. For $B \geq 1$ the Curie–Weiss model will not display SSB, not even in the classical limit. For these values of B , the well will be a single potential, as depicted in Figure 7.

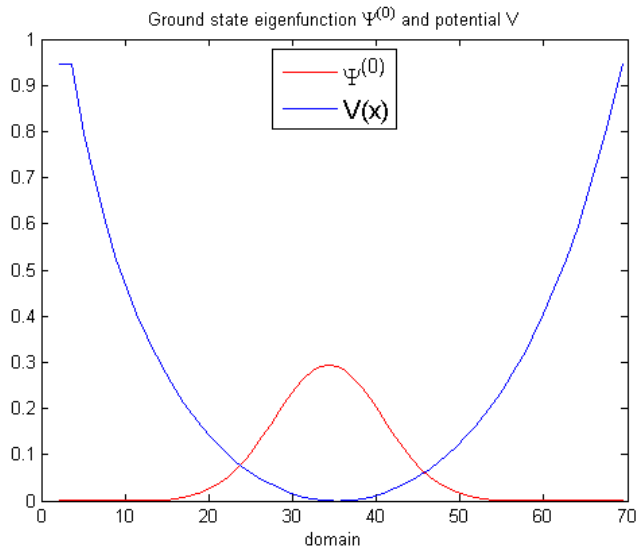


Figure 7: The scaled and shifted potential \tilde{V}_N for $B = 2$ and $J = 1$, and the ground state eigenfunction corresponding to J_{N+1}/N for $N = 60$. The single well is clearly visible. Also now, the ground state eigenvector is normalized to 1.

In view of the corresponding Schrödinger operator, the ground state in the classical limit will not break the symmetry for a single potential well, and is therefore also compatible with the Curie-Weiss model for $B \geq 1$. Note that in Figure 6 and Figure 7 some asymmetry is visible in left part of the potential. This is a result of freedom of choice one has to split the kinetic and potential energy in the first point. The same asymmetry is present in Figure 5, but due to the relative high dimension (viz. $N = 1000$), it is more difficult to visualize this asymmetry. We now return to the regime $0 \leq B < 1$. One can compute the spectral properties of the matrix J_{N+1}/N and compare them with those of the operator \tilde{H}_N . We will see that to a very good approximation the spectral properties of both matrices coincide and get better with increasing N . We have programmed the matrix \tilde{H}_N in MATLAB. The matrix has been diagonalized. The spectral properties have been compared to those of J_{N+1}/N (Table 1). In the middle column the first 10 eigenvalues of the operator \tilde{H}_N , denoted by λ_n , are displayed. Moreover, the first ten eigenvalues of the matrix J_{N+1}/N , denoted by ϵ_n , are computed, as well as the absolute difference $|\lambda_n - \epsilon_n|$ which has been displayed in the right column. The number $N = 1000$ is fixed.

Table 1. Eigenvalues and absolute differences

n	λ_n	$ \lambda_n - \epsilon_n $
0	-0.6251	3.1724×10^{-6}
1	-0.6251	3.1724×10^{-6}
2	-0.6234	2.2883×10^{-7}
3	-0.6234	2.2883×10^{-7}
4	-0.6217	7.0632×10^{-6}
5	-0.6217	7.0632×10^{-6}
6	-0.6200	1.7285×10^{-5}
7	-0.6200	1.7285×10^{-5}
8	-0.6183	3.0849×10^{-5}
9	-0.6183	3.0849×10^{-5}

We see that the first ten eigenvalues for both matrices are the same up to at least five decimals. It is also clear that these eigenvalues are doubly degenerate, at least up to four decimals.

We made a plot of the ground state eigenfunction of \tilde{H}_N as well. This function has been compared to the ground state of J_{N+1}/N . Both graphs are displayed in Figure 8. In fact, since the ground state is already numerically doubly degenerate for $N = 1000$, the computer picks a linear combination of the two eigenvectors, as already explained in §2.2. This choice depends on the algorithm, since when one changes N , the computer might pick the left located peak as a ground state as well. We forced the computer to take the right located peak for both operators in order to make the comparison. The table and the graph above show that we have strong numerical evidence that the original tridiagonal matrix may be related to \tilde{H}_N , which was not *a priori* clear since J_{N+1}/N only contains two equal sub-blocks that approximate the sub-block of order \sqrt{N} in the matrix \tilde{H}_N , viz.

$$-\frac{1}{8} [\cdot \cdot \cdot 1 \ -2 \ 1 \ \cdot \cdot \cdot] + \text{diag}(J_{N+1}/N) - \frac{1}{4}. \quad (3.46)$$

As has been numerically checked in §3.1 (see for example Figure 4), the reason is that the eigenvectors of both operators *only* localize on the specific subset of order \sqrt{N} , centered around the two minima of the double well.

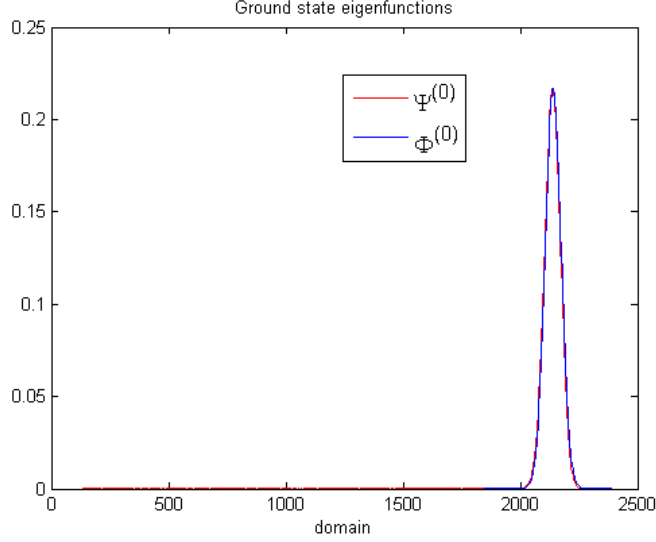


Figure 8: Both ground states plotted on the domain of order N , for $N=1000$. $\Psi^{(0)}$ corresponds to \tilde{H}_N and $\Phi^{(0)}$ to J_{N+1}/N .

We have computed the minimum of the potential, set it to zero, and subtracted this minimum from the lowest eigenvalues. These shifted eigenvalues then live in a positive potential with minimum equal to zero. For J_{N+1}/N and $N = 1000$, we now consider the eigenvalues ϵ_n of this matrix. We have already seen above that the lowest eigenvalues of J_{N+1}/N become doubly degenerate. Therefore, we identify these approximately doubly degenerate eigenstates with one single state that we denote by n . It follows that each n corresponds to two (approximately) degenerate eigenvalues, e.g., $n = 0$ corresponds to the ground state as well as the first excited state of J_{N+1}/N , $n = 1$ corresponds to the second and the third excited state, and so on. This is displayed in table 2 below.

Table 2. Shifted eigenvalues for odd values of n

n	ϵ_n
0	0.000863
1	0.002591
2	0.004310
3	0.006013
4	0.007710

Using this table, we deduce that the energy splitting is given approximately given by $\sqrt{3}/N$, when N large enough. The ground state (shifted) eigenvalue (which is approximately doubly degenerate) is then given by $\frac{1/2\sqrt{3}}{N}$, the first excited state (also approximately doubly degenerate) by $\frac{3/2\sqrt{3}}{N}$, the second excited state by $\frac{5/2\sqrt{3}}{N}$ etc. Therefore, there is excellent numerical evidence that the (approximately) doubly degenerate shifted spectrum of J_{N+1}/N is given by

$$\frac{(n + 1/2)\sqrt{3}}{N}, \quad (n = 0, 1, 2, \dots) \text{ for } N \text{ large enough.} \quad (3.47)$$

So far, both tables have been computed for fixed N , but also different values of N need to be considered. We will focus on the ground state eigenvalue ϵ_0^N of the matrix J_{N+1}/N . See Table 3:

N	$N\epsilon_0^N$
100	0.8473
1000	0.8633
2500	0.8653
5000	0.8655

Thus ϵ_0^N will approximate $\frac{1/2\sqrt{3}}{N}$ when N increases. This shows that (3.47) indeed makes sense.

What do we learn from these simulations? We started with the tridiagonal matrix J_{N+1}/N . Using a central difference approximation on a non-uniform grid, we showed that locally we had (an approximate) uniform discretization on a subset of order \sqrt{N} centered around the maxima of the Gaussian-like ground state peaks. Therefore, locally, this matrix approximates a kinetic and a potential energy, in that there exists a sub-block in the matrix J_{N+1}/N that has the form approximately given by $T + V$, as we explained in detail before. Using this fact, we constructed the matrix \tilde{H}_N . In fact, we showed that J_{N+1}/N locally approximates \tilde{H}_N . This in turn means that J_{N+1}/N applied to those vectors living on a specific subset on which the discretization was uniform, and are zero outside this set, yields approximately the same vectors as \tilde{H}_N applied to these vectors. We have seen that this set was centered around the maxima of the Gaussian-shaped ground state eigenvectors. In the construction of \tilde{H}_N we computed the potential \tilde{V}_N that had the shape of a symmetric double well. We found that the maxima of the doubly peaked Gaussian ground state correspond precisely with the minima of this potential well. Moreover, we have convincing numerical evidence that J_{N+1}/N is related to \tilde{H}_N , since also their spectral properties coincide to very good approximation. If N increases, this approximation gets better. The spectral properties of \tilde{H}_N behave like a Schrödinger operator describing a particle in a symmetric double well. This leads us to surmise that \tilde{H}_N is the discretization of a Schrödinger operator, an idea we now make precise.

3.3 Link with a Schrödinger operator on $L^2([0, 1])$

In this section, we are first going to make a link between the matrix \tilde{H}_N and an appropriate Schrödinger operator on a domain of order N , viewed as a subset of $L^2(\mathbb{R})$. We denote this operator by \tilde{h}_1 . Then we scale \tilde{h}_1 to an operator defined on $L^2([0, 1])$, which we denote by \tilde{h}_2 . This operator is the one we mentioned in the beginning of §3.2, viz. (3.33). We should remark that the fixed values of $B = 1/2$ and $J = 1$ used in the matrix entries for J_{N+1}/N determine also \tilde{H}_N and hence \tilde{h}_2 . Thus, the results derived in this section are based on these two parameters.

In §3.1 we explained how to approximate a second order differential operator with a discretization matrix using a central difference scheme. We also showed that a symmetric tridiagonal matrix with constant off- and diagonal entries can be identified with a discretization of a Schrödinger operator on a uniform grid. We now apply this procedure to the matrix \tilde{H}_N and we are going to find the corresponding Schrödinger operator that we

denoted by \tilde{h}_1 . The matrix \tilde{H}_N corresponds to a uniform grid spacing of $\sqrt{8}$ on a grid of length $\sqrt{8}N$. Applying the method explained in §3.1, it follows that we can identify \tilde{H}_N with the sum of a second order derivative $\frac{d^2}{dx^2}$ and a multiplication operator $m_{\tilde{V}_N}$ acting on the space $L^2([0, L_N])$, with $L_N = \sqrt{8}N$, i.e.,

$$\tilde{h}_1 = -\frac{d^2}{dx^2} + m_{\tilde{V}_N}, \quad (3.48)$$

where $m_{\tilde{V}_N}$ is the multiplication operator defined by \tilde{V}_N . The operator \tilde{h}_1 is the continuous analog of the matrix (3.44), but note that its domain depends on N . The operator \tilde{h}_1 is of course unbounded. It is not clear how the N -dependent potential \tilde{V}_N in (3.48) behaves when N increases, since the domain increases with N and so do the potential minima of \tilde{V}_N . Therefore, we will scale the interval by its length L_N , so that it becomes fixed. Thus scaling this interval by its length gives an operator on an interval $[0, 1]$. We denote this operator by \tilde{h}_2 . Note that the variable $y \in [0, 1]$ satisfies $y = x/L_N$, so that $dx/dy = L_N$, and hence $d/dx = \frac{1}{L_N}d/dy$. The Schrödinger operator on the unit interval is therefore given by

$$\tilde{h}_2 = -\frac{1}{8N^2} \frac{d^2}{dy^2} + m_{\tilde{V}}. \quad (3.49)$$

The potential \tilde{V} (for $B = 1/2$ and $J = 1$) is then given by the continuous function (3.34). As we have explained in the beginning of the previous subsection, it is clear that for $\hbar = 1/N$, we recognize the well-known Schrödinger operator describing a particle in a symmetric double well potential. It is also clear that \tilde{H}_N is a correct discretization of \tilde{h}_2 : a matrix of dimension N on an interval of order 1 gives a grid spacing $\Delta = 1/N$. It follows that

$$-\frac{1}{8N^2} \frac{d^2}{dy^2} \approx -\frac{1}{8N^2} \frac{[\dots 1 \ -2 \ 1 \ \dots]_N}{\Delta^2} = -\frac{1}{8} [\dots 1 \ -2 \ 1 \ \dots]_N, \quad (3.50)$$

and the latter matrix is precisely the kinetic term \tilde{T}_N in \tilde{H}_N . Thus, what connects these operators is the following:¹⁹

Claim 3.1. *The matrix \tilde{H}_N defined by (3.30) is a discretization (3.50) of the Schrödinger operator \tilde{h}_2 on an interval of order 1.*

We have seen in the previous subsection that the approximation \tilde{H}_N by J_{N+1}/N gets better with increasing N , so that one should consider \tilde{H}_N and hence \tilde{h}_2 for large N . It is well known that the ground state of the operator \tilde{h}_2 for finite N looks approximately like a doubly peaked Gaussian, where each peak is centered in one of the minima of the potential. For infinite N , these peaks will behave like delta distributions. Moreover, numerical simulations (Figure 4) show that the eigenfunctions of \tilde{H}_N live approximately on a grid of order \sqrt{N} points on the interval $[0, 1]$. Using the above discretization, we then have an order \sqrt{N} steps of $1/N$ each, so that in particular the ground state Gaussian has a width of $1/\sqrt{N}$. On the one hand, it is clear that this width will go to zero as $N \rightarrow \infty$. On the other hand, also the unit interval depends on N , as the latter has to be discretized with $N + 1$ points. The grid spacing of $1/N$

¹⁹Note that this claim is based on the fact that the number N occurring in the factor $1/N$ in front of the derivative $\frac{d^2}{dy^2}$ in (3.50) is the same as the dimension of the discretization matrix $[\dots 1 \ -2 \ 1 \ \dots]_N$.

will go to zero when $N \rightarrow \infty$, too. Therefore, the total number of points in the ground state peak living on a subset of order \sqrt{N} is

$$\frac{1/\sqrt{N}}{1/N} = \sqrt{N}. \quad (3.51)$$

Even though the ground state will behave like a delta peak when N gets larger, when discretizing the grid, the number of points in this peak increases with \sqrt{N} . In fact, due to the discretization of the grid we have a better approximation of the Gaussian ground state when N increases.

The equivalence between J_{N+1}/N and \tilde{H}_{N+1} for N large was originally obtained from a discretization based on a central difference scheme using a non-uniform grid. Moreover, we have seen that the operator \tilde{H}_{N+1} can be linked to a Schrödinger operator \tilde{h}_2 on $L^2([0, 1])$. For convenience, one can identify $1/N^2$ with \hbar^2 , for $\hbar = 1/N$ small, so that under this identification the operator is

$$\tilde{h}_2 = -\frac{\hbar^2}{8} \frac{d^2}{dx^2} + V(x). \quad (3.52)$$

It is also known (see e.g. Hellfer & Sjöstrand, 1985) that the lowest eigenstates of this Schrödinger operator are approximately degenerate when the barrier of the double well potential is sufficiently high. For such a potential, we have seen that these states approximately behave like a linear combination of weighted Hermite polynomials centered in both minima of the potential. These polynomials are given by

$$\varphi_n(x) = e^{-x^2/2} H_n(x), \quad n = 0, 1, 2, \dots \quad (3.53)$$

Thus for this type of potential, the ground state in particular is approximately given by two Gaussians, each localized in one of the minima. The spectrum of this operator consists of eigenvalues and the lowest eigenvalues are approximately doubly degenerate and equidistant in this semiclassical approach. This relies on the assumption that we can approximate both wells with a parabola, which can be justified from the WKB approximation. It can then be shown that the eigenvalues of \tilde{h}_2 are approximately given by

$$E_{n,\pm} \approx (n + 1/2)\hbar\omega \mp \hbar C e^{-\frac{1}{\hbar}\varphi}, \quad (n = 0, 1, 2, \dots). \quad (3.54)$$

where φ is an integral with positive integrand, and $C > 0$. In the case of \tilde{h}_2 we have a factor $1/N$ which now plays the role of \hbar in (3.52). Hence, as expected, we find that also now $e^{-N\varphi} \approx 0$, if N becomes large. As a result, the lowest eigenstates indeed become approximately doubly degenerate as we have already seen from the tables in §3.2.²⁰

4 The flea on Schrödinger's Cat in the Curie–Weiss model

In this section we introduce a perturbation in the quantum Curie-Weiss model h_N^{CW} such that the delocalized ground state as displayed in Figure 1 localizes already for finite N , but this time it does not do so as a result of numerical degeneracy. We compare the

²⁰This can also be justified from the WKB approximation (van de Ven, 2018, §4.8, p.66).

ground state of the perturbed Hamiltonian to the unperturbed one and again make the link with a Schrödinger operator, as explained in the previous section. We will see that the perturbation produces a small asymmetric flea on the double well potential corresponding to this Schrödinger operator. The localization of the ground state to the left or the right side of the potential barrier is a result of where exactly this flea is put. As explained in the Introduction, this accounts for the fact that real materials (which are described by the quantum theory of finite systems) do display SSB, even though the theory seems to forbid this. Indeed, these ‘flea’-like perturbations (resulting in localization of the ground state) arise naturally and might correspond to imperfections of the material.

4.1 Perturbation of the Hamiltonian

Recall the symmetrizer S_N defined in (1.9), which is a projection onto the space of all totally symmetric vectors. As we have seen, a basis for the space of totally symmetric vectors is given by the vectors $\{|n_+, n_-\rangle \mid n_+ = 0, \dots, N\}$, which spans the subspace $\text{Sym}^N(\mathbb{C}^2)$. In order to define the flea perturbation, again we may pick a basis for \mathcal{H}_N and define the perturbation on a basis for \mathcal{H}_N . Since the original Hamiltonian was defined on the standard basis β , we do the same for the perturbation. In the proof of Theorem 2.1, we have seen there is a bijection between the number of orbits and the dimension of $\text{Sym}^N(\mathbb{C}^2)$. The identification was made as follows:

$$\mathcal{O}^k \leftrightarrow |N - k, k\rangle, \quad (4.1)$$

where k in $|N - k, k\rangle$ labels the number of occurrences of the vector e_2 in any of the basis vectors $\beta_i \in \beta$, and $N - k$ in $|N - k, k\rangle$ labels the occurrence of the vector e_1 in β_i , so that $N - k$ stands for the number of spins in the up direction whilst the second position k denotes the number of down spins. By definition of the Symmetrizer S_N , any basis vector $\beta_k \in \beta$ in the same orbit \mathcal{O}^k will be mapped under S_N to the same vector in $\text{Sym}^N(\mathbb{C}^2)$, which equals

$$\frac{1}{\sqrt{\binom{N}{k}}} \sum_{l=1}^{\binom{N}{k}} \beta_{k_l}. \quad (4.2)$$

Here the suffix l in β_{k_l} labels the basis vector $\beta_k \in \beta$ within the same orbit \mathcal{O}^k . So for each orbit \mathcal{O}^k , we have $\binom{N}{k}$ vectors β_k . Hence for each $l = 1, \dots, \binom{N}{k}$ the image $S_N(\beta_{k_l})$ under S_N is always the same, namely the coordinate vector written with respect to β . It turns out that the perturbation we are going to define will be very similar to the Symmetrizer operator. Of course, since we have expressed our original Curie-Weiss Hamiltonian with respect to this $|n_+, n_-\rangle$ -basis, we need to do the same for the perturbation we are going to define now. Since we have a partition of our 2^N -dimensional basis β into $N + 1$ orbits, we define a perturbation as follows: we fix $k \in \{0, \dots, N\}$ as well as some real number λ_k dependent of k . We denote the perturbation by $V_{\lambda_k}^k$. Then by definition of this perturbation any basis vector β_{k_l} in the corresponding orbit \mathcal{O}^k will be mapped to

$$V_{\lambda_k}^k : \beta_{k_l} \mapsto \lambda_k S_N(\beta_{k_l}), \quad \left(l = 1, \dots, \binom{N}{k} \right). \quad (4.3)$$

All other $2^N - \binom{N}{k}$ basis vectors β_i will be sent to $S_N(\beta_i)$. The parameter λ_k is a real number that denotes the strength of the perturbation. When we transform the matrix $[V_{\lambda_k}^k]_{\beta}$ in the

β basis to the matrix written in the $|n_+, n_-\rangle$ - basis, it is obvious that it becomes a diagonal matrix with the value λ_k at entry (k, k) . If we can show that $V_{\lambda_k}^k$ commutes with S_N and that the ground state eigenvector of the perturbed Hamiltonian $h_N + V_{\lambda_k}^k$ is unique, then we may conclude that the ground state lies in the subspace $\text{Sym}^N(\mathbb{C}^2)$. The reason for this is the same as for the unperturbed Curie-Weiss Hamiltonian: these properties push this eigenvector into the subspace $\text{ran}(S_N) = \text{Sym}^N(\mathbb{C}^2)$, so that we may diagonalize this Hamiltonian represented as a matrix that can be written with respect to the symmetric subspace, which will be a tridiagonal matrix of dimension $N+1$ as well. This makes computations much easier, and allows one to compare both systems, i.e. the unperturbed one and the perturbed one. Similarly as for the Curie-Weiss model, a sufficient condition for uniqueness of the ground state of the perturbed matrix, originally written with respect to the standard basis for \mathcal{H}_N , is non-negativity and irreducibility, so that we can apply the Perron–Frobenius Theorem, as explained in Appendix A. This depends, of course, on the parameter λ_k . We will come back to this later. In order to show that the commutator is zero, i.e., $[S_N, V_{\lambda_k}^k] = 0$, it suffices to show this for a basis. We check it for the standard basis β of the N -fold tensor product. Fix a basis vector β_j in \mathcal{O}^k . If we take any basis vector β_i not in \mathcal{O}^k , then

$$V_{\lambda_k}^k S_N(\beta_i) = S_N^2(\beta_i) = S_N(\beta_i), \quad (4.4)$$

since the symmetrizer cannot map β_i into the orbit \mathcal{O}^k . If we take any vector β_i in \mathcal{O}^k , then

$$\begin{aligned} V_{\lambda_k}^k S_N(\beta_i) &= V_{\lambda_k}^k \frac{1}{\sqrt{\binom{N}{k}}} \sum_{l=1}^{\binom{N}{k}} \beta_{i_l} = \frac{1}{\sqrt{\binom{N}{k}}} \sum_{l=1}^{\binom{N}{k}} V_{\lambda_k}^k(\beta_{i_l}) \\ &= \frac{\lambda_k}{\sqrt{\binom{N}{k}}} \sum_{l=1}^{\binom{N}{k}} S_N(\beta_{i_l}) = \lambda_k S_N^2(\beta_i) = \lambda_k S_N(\beta_i). \end{aligned} \quad (4.5)$$

since $S_N(\beta_i)$ lies in the orbit \mathcal{O}^k and thus is a linear combination of all other $\binom{N}{k}$ vectors in this orbit. On the other hand, if we take any basis vector β_i not in \mathcal{O}^k , then again as before,

$$S_N V_{\lambda_k}^k(\beta_i) = S_N^2(\beta_i) = S_N(\beta_i), \quad (4.6)$$

since $V_{\lambda_k}^k$ acts as the Symmetrizer on vectors in $\text{ran}(S_N) = \text{Sym}^N(\mathbb{C}^2)$ that are not equal to β_j . Finally, if we take any vector β_i in \mathcal{O}^k then,

$$S_N V_{\lambda_k}^k(\beta_i) = S_N \lambda_k S_N(\beta_i) = \lambda_k S_N(\beta_i). \quad (4.7)$$

Thus we see that for all basis vectors $\beta_i \in \beta$ we have $[S_N, V_{\lambda_k}^k](\beta_i) = 0$. The last step is to show that the Hamiltonian $-(h_N + V_{\lambda_k}^k)$, written with respect to the standard basis β for \mathcal{H}_N , is a non-negative and irreducible matrix. Since the off-diagonal elements are completely determined by the unperturbed Hamiltonian and are never zero, the matrix can never be decomposed into two blocks, so that it remains irreducible. Non-negativity is achieved when

$$\frac{J}{2N}(2n_+ - N)^2 - \lambda_{n_+} \geq 0. \quad (4.8)$$

This depends of course on $k = n_+$ and hence on the orbit \mathcal{O}^{n_+} where we have put the perturbation. Any $V_{\lambda_{n_+}}^{n_+}$ satisfying this inequality guarantees non-negativity. If we assume

that this is satisfied, then together with the fact that $h_N + V_{\lambda_{n_+}}^k$ commutes with S , in the same spirit as for the unperturbed Curie-Weiss model we can conclude that the ground state of the perturbed Hamiltonian is unique, and therefore indeed lies in $\text{ran}(S_N) = \text{Sym}^N(\mathbb{C}^2)$. Finally, knowing now that we may diagonalize the perturbed Hamiltonian with respect to the symmetric basis $|n_+, n_-\rangle$, we use the fact that the sum of two linear transformations written with respect to a basis individually equals the sum of both linear transformations if this total sum is written with respect to the basis, i.e.:

$$[h_N]_{|n_+, n_-\rangle} + [V_{\lambda_k}^k]_{|n_+, n_-\rangle} = [h_N + V_{\lambda_k}^k]_{|n_+, n_-\rangle}. \quad (4.9)$$

Therefore, since we may diagonalize $h_N + V_{\lambda_k}^k$ in the symmetric basis $|n_+, n_-\rangle$, the above observation (4.9) ensures that it suffices to diagonalize the sum of the individual matrices represented in this basis, i.e., the tridiagonal matrix $[h_N]_{|n_+, n_-\rangle}$ (viz. (2.1)) and the perturbation matrix $[V_{\lambda_k}^k]_{|n_+, n_-\rangle}$.

Recall that in §2.2 the ground state $\psi_N^{(0)}$ of the unperturbed Hamiltonian h_N^{CW} was approximately given by two Gaussians (for N large), each of them located in one of the wells of the potential, and was given by

$$\psi_N^{(0)} \cong \frac{T_a(\varphi_0) + T_{-a}(\varphi_0)}{\sqrt{2}}. \quad (4.10)$$

In fact, this is true for any finite N , since the ground state is unique. However, due to numerical degeneracy of the ground state and the first excited state for about $N \geq 80$, these two states will form a linear combination χ_{\pm} given by (2.18). By a simple calculation, we found that for these relative large values of N , the (numerical) degenerate ground state is given by

$$\chi_{\pm} \cong T_{\pm a}(\varphi_0), \quad (4.11)$$

where the functions $\varphi_0(x)$ have to be understood as functions on a discrete grid. For $N < 80$, we observed that a plot of the ground state displayed a doubly peaked Gaussian, as expected from (4.10). This made sense, since the energy levels in the latter case are not degenerate, not even for the computer. As we have mentioned we wanted to show that, due to the perturbation, the (unique) ground state localizes for finite N . We have just argued that this happens already for $N \geq 80$, but this was a result of numerical inaccuracy/degeneracy. The question is then if our perturbation forces the ground state to localize for finite N in such a way that it will be not a result of numerical degeneracy. The answer is yes. It depends on the parameter λ_{n_+} with n_+ denoting the n_+^{th} position in the diagonal matrix of the perturbation. Completely analogously as in section 3, we can extract the potential corresponding to the perturbed Hamiltonian $h_N + V_{\lambda_{n_+}}^k$, written with respect to the symmetric basis. We scaled this Hamiltonian by $1/N$ and translated the potential so that its minima are set to zero. We have made a plot of this potential (Figure 9). For convenience, we scaled the domain to the unit interval. Moreover, we plotted the ground state of this Hamiltonian and the one corresponding to the unperturbed one (Figure 10). We observe a localization of the ground state in the right sided well. Simulations showed that the eigenvalues of the perturbed Hamiltonian are non-degenerate, so that the ground state is indeed unique, also for the computer. Hence, the localization is not a result of numerical degeneracy. We did a similar simulation for this ‘flea’ perturbation, but now located on the right site of the barrier

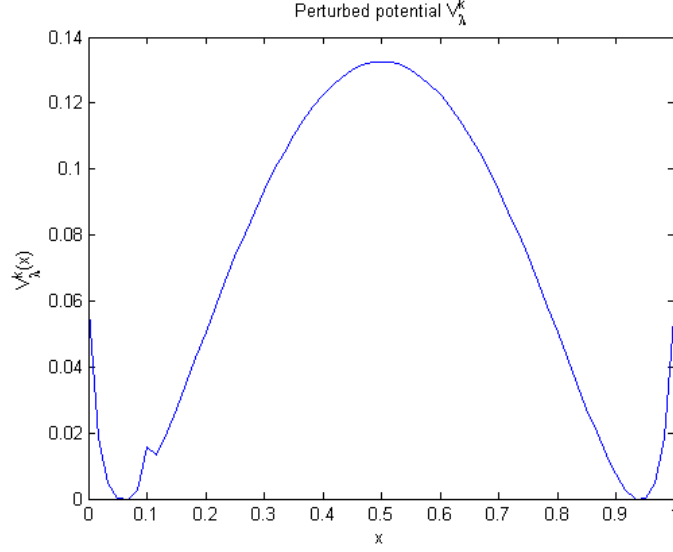


Figure 9: The perturbed potential energy computed from the tridiagonal matrix $h_N^{CW} + V_{\lambda_k}^k$ for $N = 60$, $\lambda_k = 0.5$, $k = 7$, $J = 1$ and $B = 1/2$. This potential has a ‘flea’ on the left side of well due the perturbation $V_{\lambda_k}^k$.

(Figure 11). We see a localization of the ground state to the left side of the barrier (Figure 12). Our conclusion is that due to this ‘flea’-like perturbation, the ground state will localize in one of the wells depending on where the flea is put. This localization may be understood from energetic considerations. For example, if $\lambda_{n_+} > 0$ such that condition (4.8) is satisfied and the perturbation is located on the right, then the relative energy in the left-hand part of the double well is lowered, so that localization will be to the left. This result matches exactly the work done in Landsman & Reuvers (2013), where the Schrödinger operator with a symmetric double well was studied rather than quantum spin systems, and confirms the analogy between these models already noted by Landsman (2013, 2017).

The last topic of this section is to relate these results to symmetry breaking. Given the perturbed Hamiltonian $h_N + V_{\lambda_k}^k$ such that (4.8) is satisfied, we know that the unique ground state lies in $\text{Ran}(S_N) = \text{Sym}^N(\mathbb{C}^2)$. However, we do not have a \mathbb{Z}_2 -symmetry of the system since this perturbed Hamiltonian does not commute with the unitary operator $u^{(N)} = \otimes_{x=1}^N \sigma_1(x)$ implementing this \mathbb{Z}_2 -symmetry. The following result is obvious, but we state it for completeness and without proof.

Proposition 4.1. *The unitary operator $u^{(N)} = \otimes_{x=1}^N \sigma_1(x)$ does not commute with $V_{\lambda_k}^k$, and therefore the ground state of the perturbed Hamiltonian $h_N + V_{\lambda_k}^k$ is not \mathbb{Z}_2 -invariant.*

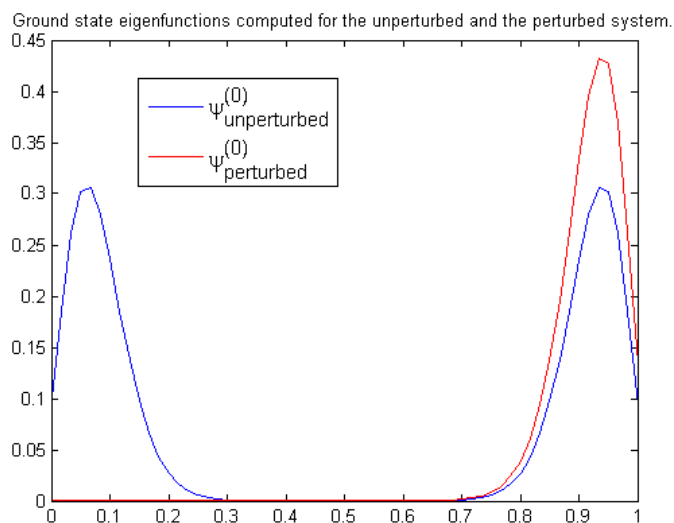


Figure 10: The corresponding ground state (in red) of the perturbed Hamiltonian $h_N^{CW} + V_{\lambda_k}^k$ is already localized for $N = 60$, $\lambda_k = 0.5$, $k = 7$, $J = 1$ and $B = 1/2$. For these values of λ_k and k , still condition (4.8) is satisfied. The localization takes place on the right side of the well, since the flea lifts the potential on the left side.

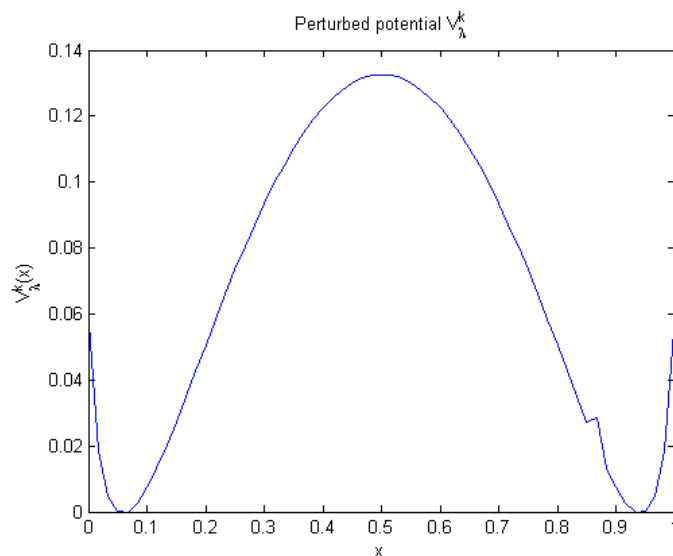


Figure 11: The perturbed potential energy computed from the tridiagonal matrix $h_N^{CW} + V_{\lambda_k}^k$ for $N = 60$, $\lambda_k = 0.5$, $k = 7$, $J = 1$ and $B = 1/2$. This potential has a ‘flea’ on the right side of the well due the perturbation $V_{\lambda_k}^k$.

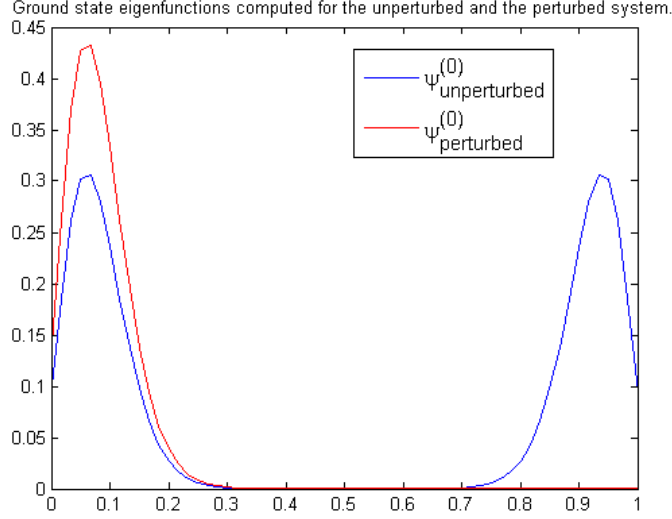


Figure 12: The corresponding ground state (in red) of the perturbed Hamiltonian $h_N^{CW} + V_\lambda^k$ is already localized for $N = 60$, $\lambda_k = 0.5$, $k = N - 7$, $J = 1$ and $B = 1/2$. For these values of λ_k and k , condition (4.8) is still satisfied. Localization takes place on the left side of the barrier, since the flea lifts the potential on the right side.

5 Conclusion

We have established a link between the quantum Curie-Weiss Hamiltonian and a one $1d$ Schrödinger operator describing a particle in a symmetric double well potential for $\hbar > 0$, where $\hbar = 1/N$. We have shown that the scaled quantum Curie-Weiss Hamiltonian restricted to the $(N+1)$ -dimensional subspace $\text{Sym}^N(\mathbb{C}^2)$ approximates a discretization matrix corresponding to this Schrödinger operator, defined on $L^2([0, 1])$. Subsequently, we have shown that due to a small perturbation a \mathbb{Z}_2 -symmetry of the Curie-Weiss model can already be explicitly broken for finite N , resulting in a pure ground state in the classical limit. This form of *explicit* symmetry breaking due to a small perturbation has also been studied from a similar perspective for the Schrödinger operator with a symmetric double well potential (e.g. “flea on the elephant”), as indicated in the abstract. We have seen that those results were completely in accordance with our findings regarding the Curie-Weiss model. However, more research needs to be done to prove analytically (rather than infer from numerical simulations) the connection between the Schrödinger operator and the quantum Curie-Weiss model. For example, one should prove that the ground state eigenfunction of the restricted Curie-Weiss Hamiltonian localizes on a subset of order \sqrt{N} . Apart from that, another open problem is that we do not know if the excited states of the Curie-Weiss Hamiltonian defined on $\bigotimes_{n=1}^N \mathbb{C}^2$ are in the symmetric subspace or not; we only know this for the ground state. Therefore, considering the tridiagonal matrix, one may not *a priori* conclude that for example the first excited state of this matrix corresponds also to the first excited state of the original Curie-Weiss Hamiltonian. This raises the general question if there are more quantum spin systems that can be related to Schrödinger operators with some potential and vice versa. As for the quantum-Curie-Weiss model, the crucial property is the existence of a subspace of $\bigotimes_{n=1}^N \mathbb{C}^2$ and a basis such that the spin Hamiltonian, written with respect to this basis of the subspace, is a tridiagonal matrix.

A Perron–Frobenius Theorem

In this appendix we provide the machinery for proving the uniqueness of the ground state of the Curie–Weiss model for any finite N , based on the Perron-Frobenius Theorem. Though the result is well known, the precise combination of arguments is hard to find in the literature. We start with some definitions and basis facts.

- Definition A.1.**
1. A square matrix is called *non-negative* if all its entries are non-negative. It is called *strictly positive* if all its entries are strictly positive.
 2. A non-negative matrix a is called *irreducible* if for every pair indices i and j there exists a natural number m such that $(a^m)_{ij}$ is not equal to zero. If the matrix is not irreducible, it is said to be reducible.
 3. A *directed graph* is a graph $G = (V, E)$ with vertices V and edges E such that the vertices are connected by the edges, and where the edges have a direction. A directed graph is also called a *digraph*.
 4. A digraph is called *strongly connected* if there is a directed path x to y between any two vertices x, y .

We use the notion of the directed graph or digraph of a square N -dimensional matrix a , denoted by $G(a)$. We say that the digraph of a is the digraph with

$$V = \{1, 2, \dots, N\},$$

$$E = \{(i, j) \mid a_{ij} \neq 0\}.$$

The following result links irreducibility of a non-negative matrix to strongly connectedness of its corresponding digraph. The proof is easy and therefore omitted.

Lemma A.2. *A non-negative square matrix a is irreducible if and only if the digraph of a is strongly connected.*

We now come to the Perron-Frobenius Theorem. There are two versions of this theorem: one for *strictly positive* matrices, and the other for *irreducible* matrices. We use the version for irreducible matrices since the Curie-Weiss Hamiltonian $-h_N^{CW}$, represented with respect to the standard basis for $\bigotimes_{n=1}^N \mathbb{C}^2$, is a non-negative and irreducible matrix of dimension 2^N , as we will see below.

Theorem A.3. *Let a be an $N \times N$ real-valued non-negative matrix, and denote its spectral radius by $r(a) = \lambda$. If a is irreducible, then $\lambda = r(a)$ an eigenvalue of a , which is positive, simple, and corresponds to a strictly positive eigenvector.*

This theorem is based on properties of a matrix relative to some basis, so that the Perron-Frobenius Theorem is valid if there exists a basis such that the matrix representation of the operator in this basis satisfies the assumptions of the theorem. Note that multiplying $-h_N^{CW}$ by -1 , the eigenvalues will change sign and we find instead that the smallest eigenvalue (i.e. the ground state) of h_N^{CW} is simple and corresponds to a strictly positive eigenvector. As a case in point, we are now going to prove a statement about our Hamiltonian $-h_N^{CW}$, relative to the standard basis of \mathbb{C}^2 extended to a basis of the tensor product $\bigotimes_{n=1}^N \mathbb{C}^2$ in the usual way.

Theorem A.4. *The Curie-Weiss Hamiltonian $-h_N^{CW}$ from (1.5), represented in the standard basis for $\bigotimes_{n=1}^N \mathbb{C}^2$, is non-negative and irreducible.*

Proof. Since all constant factors in $-h_N^{CW}$ are strictly positive, we only have to consider both terms containing sums. We show that

$$\sum_{x,y \in \Lambda_N} \sigma_3(x)\sigma_3(y) \quad \text{and} \quad \sum_{x \in \Lambda_N} \sigma_1(x) \quad (\text{A.1})$$

are non-negative. We have seen in the proof of Theorem 2.1 that the operator $\sum_{x,y \in \Lambda_N} \sigma_3(x)\sigma_3(y)$ is a diagonal matrix with respect to the standard basis $\{e_{n_1} \otimes \dots \otimes e_{n_N}\}_{n_1=1, \dots, n_N=1}^2$ for $\bigotimes_{n=1}^N \mathbb{C}^2$. For non-negativity we must prove, independently of the basis vectors, that there are at least as many plus signs as there are minus signs, i.e., we have to show that

$$N^2 - 2n_+(N - n_+) \geq 2n_+(N - n_+). \quad (\text{A.2})$$

This gives $N^2 - 4n_+(N - n_+) \geq 0$ if and only if $N^2 - 4Nn_+ + 4n_+^2 \geq 0$. The parabola $n_+ \mapsto N^2 - 4n_+N + 4n_+^2$ attains its minimum in $n_+ = N/2$, which is given by $N^2 - 4(\frac{N}{2})N + 4(\frac{N}{2})^2 = 0$. So indeed, there are at least as many plus signs as minus signs, so that the corresponding diagonal term is non-negative. The other term $\sum_{x \in \Lambda_N} \sigma_1(x)$ does not contain any negative entries at all, so if we apply this to any basis vector $\{e_{n_1} \otimes \dots \otimes e_{n_N}\}$, we get a non-negative matrix. It follows that both operators in (A.1) are non-negative in the basis under consideration.

Now we show that the matrix corresponding to the Curie-Weiss Hamiltonian is irreducible. Note that irreducibility of a matrix does not depend on the basis in which the operator is represented, since similar matrices define equivalent representations which preserve irreducibility. We use Lemma A.2 to show that there is a direct path between any two vertices. But this is obvious: the operator $\sum_x \sigma_1(x)$ flips the spins one by one, and therefore the associated digraph is clearly strongly connected as we can find a directed path between any two vertices.²¹ \square

By the Perron-Frobenius Theorem, the largest eigenvalue of the Curie-Weiss Hamiltonian $-h_N^{CW}$ is positive, simple and corresponds to a strictly positive eigenvector. This in turn implies that the ground state eigenvalue of h_N^{CW} is positive, simple, and has a strictly positive eigenvector.

B Discretization

This information provided in this appendix is based on Kuzmin (2017), Kajishima & Taira (2017), G.C. Groenenboom (1990), and Sundqvist (1970). These results have been used in §3.1.

Recall from calculus that the following approximations are valid for the derivative of single-variable functions $f(x)$. The first one is called the forward difference approximation and is an expression of the form

$$f'(x) = \frac{f(x+h) - f(x)}{h} + O(h) \quad (h > 0). \quad (\text{B.1})$$

²¹A different proof is given in van de Ven (2018), §5.3, p.78.

The backward difference approximation is of the form

$$f'(x) = \frac{f(x) - f(x-h)}{h} + O(h) \quad (h > 0). \quad (\text{B.2})$$

Furthermore, the central difference approximation is

$$f'(x) = \frac{f(x+h) - f(x-h)}{2h} + O(h^2) \quad (h > 0). \quad (\text{B.3})$$

The approximations are obtained by neglecting the error terms indicated by the O-notation. These formulas can be derived from a Taylor series expansion around x ,

$$f(x+h) = f(x) + hf'(x) + \frac{h^2}{2}f''(x) + \dots = \sum_{n=0}^{\infty} \frac{h^n}{n!} f^{(n)}(x), \quad (\text{B.4})$$

and

$$f(x-h) = f(x) - hf'(x) + \frac{h^2}{2}f''(x) - \dots = \sum_{n=0}^{\infty} (-1)^n \frac{h^n}{n!} f^{(n)}(x), \quad (\text{B.5})$$

where $f^{(n)}$ is the n^{th} order derivative of f . Subtracting $f(x)$ from both sides of the above two equations and dividing by h respectively $-h$ leads to the forward difference respectively the backward difference. The central difference is obtained by subtracting equation (B.5) from equation (B.4) and then dividing by $2h$.

The question is how small h has to be in order for the algebraic difference $\frac{f(x+h)-f(x)}{h}$ (i.e. in this case the forward difference approximation) to be good approximation of the derivative. It is clear from the above formulas that the error for the central difference formula is $O(h^2)$. Thus, central differences are significantly better than forward and backward differences. Higher order derivatives can be approximated using the Taylor series about the value x

$$f(x+2h) = \sum_{n=0}^{\infty} \frac{(2h)^n}{n!} f^{(n)}(x) \quad (\text{B.6})$$

and

$$f(x-2h) = \sum_{n=0}^{\infty} (-1)^n \frac{(2h)^n}{n!} f^{(n)}(x). \quad (\text{B.7})$$

A forward difference approximation to $f''(x)$ is then

$$\frac{f(x+2h) - 2f(x+h) + f(x)}{h^2} + O(h), \quad (\text{B.8})$$

and a centered difference approximation is for example

$$\frac{f(x+h) - 2f(x) + f(x-h)}{h^2} + O(h^2). \quad (\text{B.9})$$

Now we discretize the kinetic and potential energy operator. For simplicity, consider the one-dimensional case. We first discretize the interval $[0, 1]$ using a uniform grid of N points

$x_i = ih, h = \frac{1}{N}, i = 0, 1, \dots, N$. It follows that $f(x) \mapsto f(x_i) =: f_i$. The Taylor series expansion of a function about a point x_i becomes

$$f_{i+k} = f_i + \sum_{n=0}^{\infty} (-1)^n \frac{(kh)^n}{n!} f^{(n)}(x), \quad (\text{B.10})$$

where $k = \pm 1, \pm 2, \dots, \pm N$. Similar as above, we can find central difference formulas for f'_j, f''_j , namely

$$f'_j = \frac{-f_{j-1} + f_{j+1}}{2h} + O(h^2) \quad (\text{B.11})$$

$$f''_j = \frac{f_{j-1} - 2f_j + f_{j+1}}{h^2} + O(h^2). \quad (\text{B.12})$$

The approximations are again obtained by neglecting the error terms.

Using this uniform grid with grid spacing $h = 1/N$, it follows that the second derivative operator in one dimension is given by the tridiagonal matrix $\frac{1}{h^2}[\dots 1 \ -2 \ 1 \ \dots]_N$ and the potential which acts as multiplication, is given by a diagonal matrix. With the notation $\frac{1}{h^2}[\dots 1 \ -2 \ 1 \ \dots]_N$, we mean the N -dimensional matrix

$$\frac{1}{h^2} \begin{pmatrix} -2 & 1 & & & \\ 1 & -2 & 1 & & 0 \\ & \ddots & \ddots & \ddots & \\ & & 0 & 1 & -2 & 1 \\ & & & & 1 & -2 \end{pmatrix}.$$

Now suppose that the values of the kinetic energy operator T are non-uniformly dependent of the positions in space. Then one needs to use a non-uniform grid in order to get a good description of the second derivative. We use the central difference approximation and approach f by a Taylor series.

Denote x_j by the j^{th} grid point and $f_k = f(x_k)$. Then the Taylor series of f at x_j can be written as

$$f_k = f_j + \sum_{m=1}^{\infty} \frac{(x_k - x_j)^m}{m!} f_j^{(m)}. \quad (\text{B.13})$$

If we let $h_j = x_{j+1} - x_j$, then similarly as above, for a three-point finite-difference formula i.e., only f_{i+1}, f_i, f_{i-1} are used, we find that

$$f_{j+1} = f_j + h_j f'_j + \frac{h_j^2}{2} f''_j + \frac{h_j^3}{6} f_j^{(3)} + \dots \quad (\text{B.14})$$

and similarly one can write $x_{j-1} = x_j - h_{j-1}$, so that we find

$$f_{j-1} = f_j - h_{j-1} f'_j + \frac{h_{j-1}^2}{2} f''_j - \frac{h_{j-1}^3}{6} f_j^{(3)} + \dots \quad (\text{B.15})$$

Both expressions can be used to eliminate f'_j to derive an expression for the second derivative:

$$f''_j = \frac{2f_{j-1}}{h_{j-1}(h_{j-1} + h_j)} - \frac{2f_j}{h_{j-1}h_j} + \frac{2f_{j+1}}{h_j(h_{j-1} + h_j)} + \frac{h_j - h_{j-1}}{3} f_j^{(3)} + \mathcal{O}(h^2). \quad (\text{B.16})$$

This is the central difference approximation for the non-uniform grid. If we assume that $h_j - h_{j-1}$ is small, we may neglect the last term, and we get precisely that

$$\frac{2}{h_{j-1}(h_{j-1} + h_j)} = T_{j,j-1}, \quad (\text{B.17})$$

$$\frac{-2}{h_{j-1}h_j} = T_{j,j}, \quad (\text{B.18})$$

$$\frac{2}{h_j(h_{j-1} + h_j)} = T_{j,j+1}. \quad (\text{B.19})$$

Therefore we find that the ratio, say ρ_j , equals

$$\rho_j = \frac{T_{j,j+1}}{T_{j,j-1}} = \frac{h_{j-1}}{h_j}. \quad (\text{B.20})$$

Thus $h_{j-1} = \rho_j h_j$. We derive from this combined with the above three equations that

$$h_j^2 = \frac{2}{T_{j,j-1}\rho_j(1 + \rho_j)}, \quad (\text{B.21})$$

$$\text{or } h_j^2 = \frac{2}{T_{j,j+1}(1 + \rho_j)}. \quad (\text{B.22})$$

References

- [1] A. E. Allahverdyana, R. Balian, and Th. M. Nieuwenhuizen, *Understanding quantum measurement from the solution of dynamical models*, Physics Reports **525**, 1–166 (2013), doi:10.1016/j.physrep.2012.11.001.
- [2] P. W. Anderson, *More is different*, Science **177**, 393–396 (1972), <https://www.jstor.org/stable/1734697>.
- [3] P. Bona, *The dynamics of a class of mean-field theories*, Journal of Mathematical Physics **29**, 2223–2235 (1988), doi:10.1063/1.528152.
- [4] J. Butterfield, *Less is different: Emergence and reduction reconciled*, Foundations of Physics **41**, 1065–1135 (2011), doi:10.1007/s10701-010-9516-1.
- [5] N. G. Duffield and R. F. Werner, *Local dynamics of mean-field quantum systems*, Helvetica Physica Acta **65**, 1016–1054 (1992), doi:10.5169/seals-116521.
- [6] J. Earman, *Curie’s Principle and spontaneous symmetry breaking*, International Studies in the Philosophy of Science **18**, 173–198 (2004), doi:10.1080/0269859042000311299.
- [7] G. C. Groenenboom and H. M. Buck, *Solving the time-independent Schrödinger equation with the Lanczos procedure*, Journal of Chemical Physics. **92**, 4374–4379 (1990), doi:10.1063/1.458575.
- [8] B. Helffer and J. Sjöstrand, *Puits multiples en limite semi-classique. II. Interaction moléculaire. Symétries. Perturbation*, Annales de l’Institut Henri Poincaré Physique Théorique **42**, 127–212 (1985), <http://eudml.org/doc/76277>.

- [9] K. Hepp, *Quantum theory of measurement and macroscopic observables*, Helvetica Physica Acta **45**, 237–248 (1972), doi:10.5169/seals-114381.
- [10] G. Jona-Lasinio, F. Martinelli, and E. Scoppola, *New approach to the semiclassical limit of quantum mechanics*, Communications in Mathematical Physics **80**, 223–254 (1981), doi:10.1007/BF01213012.
- [11] T. Kajishima and K. Taira, *Computational fluid Dynamics* (Springer, 2017), doi:10.1007/978-3-319-45304-0.
- [12] T. Koma and H. Tasaki, *Symmetry breaking and finite-size effects in quantum many-body systems*, Journal of Statistical Physics **76**, 745–803 (1994), doi:10.1007/BF02188685.
- [13] D. Kuzmin, *Introduction to CFD, lecture 4: Finite difference method* (2017), www.mathematik.uni-dortmund.de/~kuzmin/cfdintro/lecture4.pdf.
- [14] N. P. Landsman, *Mathematical Topics Between Classical and Quantum Mechanics* (Springer, 1998), doi:10.1007/978-1-4612-1680-3.
- [15] N. P. Landsman, Spontaneous symmetry breaking in quantum systems: Emergence or reduction?, *Studies in History and Philosophy of Modern Physics* **44**, 379–394 (2013), doi:10.1016/j.shpsb.2013.07.003.
- [16] N. P. Landsman, *Foundations of Quantum Theory: From Classical Concepts to Operator Algebras* (Springer Open, 2017), doi:10.1007/978-3-319-51777-3.
- [17] N. P. Landsman and R. Reuvers, *A flea on Schrödinger’s Cat*, Foundations of Physics **43**, 373–407 (2013), doi:10.1007/s10701-013-9700-1.
- [18] G. A. Raggio and R. F. Werner, *Quantum statistical mechanics of general mean field systems*, Helvetica Physica Acta **62**, 980–1003 (1989), doi:10.5169/seals-116175.
- [19] B. Simon, *Semiclassical analysis of low lying eigenvalues. IV. The flea on the elephant*, Journal of Functional Analysis **63**, 123–136 (1985), doi:10.1016/0022-1236(85)90101-6.
- [20] H. Sundqvist and G. Veronis, *A simple finite-difference grid with non-constant intervals*, Tellus **22**, 26–31 (1970), doi:10.1111/j.2153-3490.1970.tb01933.x.
- [21] C. J. F. van de Ven, *Properties of quantum spin systems and their classical limit* (M.Sc. Thesis, Radboud University, 2018), <http://www.math.ru.nl/~landsman/Chris2018.pdf>.
- [22] J. van Wezel, *Quantum Mechanics and the Big World*, PhD Thesis (Leiden University, 2007), <https://openaccess.leidenuniv.nl/handle/1887/11468>.
- [23] J. van Wezel, *Quantum dynamics in the thermodynamic limit*, Physical Review **B78**, 054301, doi:10.1103/PhysRevB.78.054301.
- [24] J. van Wezel and J. van den Brink, *Spontaneous symmetry breaking in quantum mechanics*, American Journal of Physics **75**, 635–638 (2007), doi:10.1119/1.2730839.
- [25] W. F. Wreszinski and V. A. Zagrebnoy, *Bogoliubov quasi-averages: spontaneous symmetry breaking and algebra of fluctuations*, Theoretical and Mathematical Physics **194**, 157–188 (2018), doi:10.1134/S0040577918020010.